Enhanced dipole strength and its consequences for reaction rates

Ronald Schwengner

Institut für Strahlenphysik, Helmholtz-Zentrum Dresden-Rossendorf
01314 Dresden, Germany

- Photon-scattering experiments
- Data analysis and results
- Model predictions for dipole strength
- Calculations of reaction rates using statistical models
- Photoactivation experiments

Supported by Deutsche Forschungsgemeinschaft

HZDR
HELMHOLTZ ZENTRUM DRESDEN ROSSENDORF

Mitglied der Helmholtz-Gemeinschaft

Dipole strength below to the particle-separation energy

- Modelling of astrophysical processes:
  - (γ,n) reaction rates in the p-process.
  - (n,γ) reaction rates in the s-process.

- Studies for future nuclear-fuel cycles:
  - Improved experimental and theoretical description of (n,γ) reactions.

- Open problems:
  - Differences between analytic approximations for dipole strength functions.
  - Discrepancies between strength functions deduced from experiments using different reactions.
  - Influence of nuclear deformation etc. on strength functions.

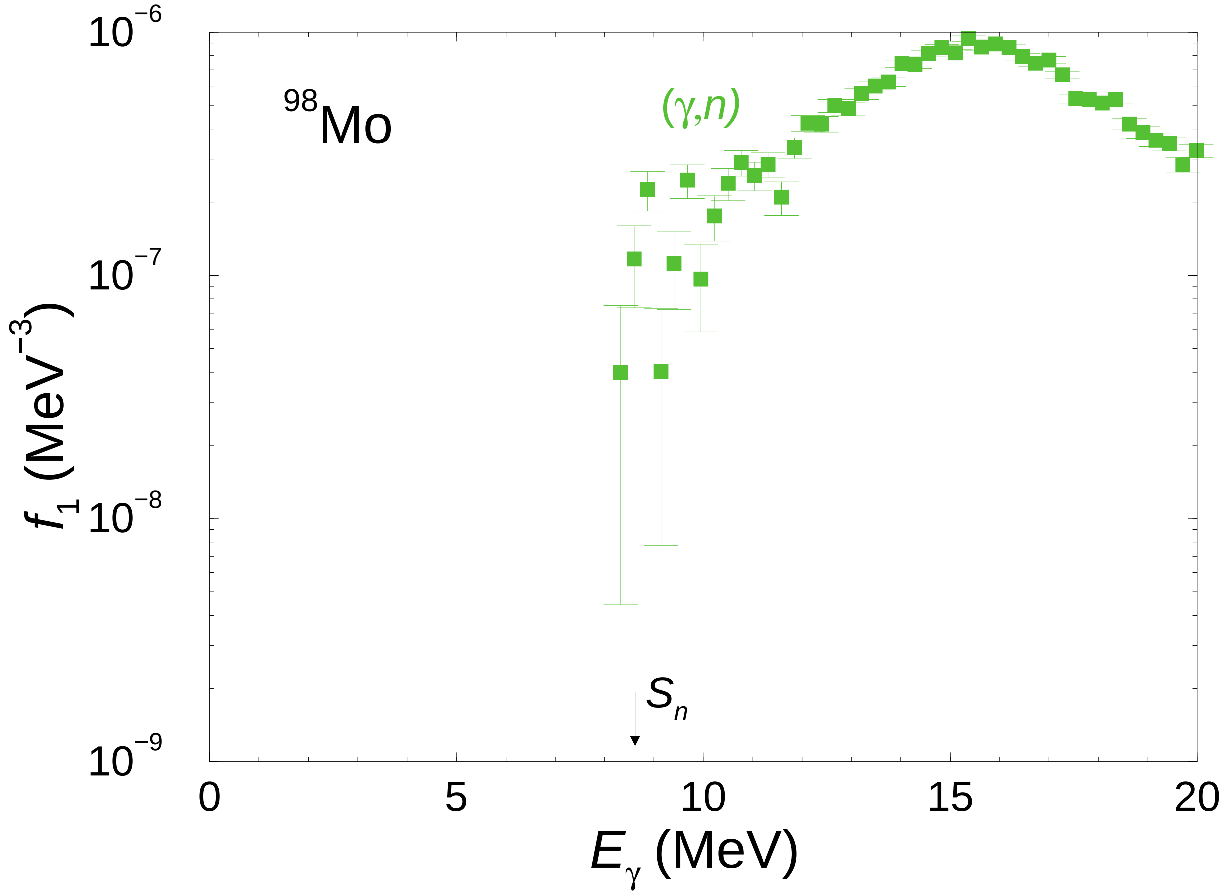

Dipole strength below to the particle-separation energy

- Modelling of astrophysical processes:
  - (γ,n) reaction rates in the p-process.
  - (n,γ) reaction rates in the s-process.
- Studies for future nuclear-fuel cycles:
  - Improved experimental and theoretical description of (n,γ) reactions.
- Open problems:
  - Differences between analytic approximations for dipole strength functions.
  - Discrepancies between strength functions deduced from experiments using different reactions.
  - Influence of nuclear deformation etc. on strength functions.

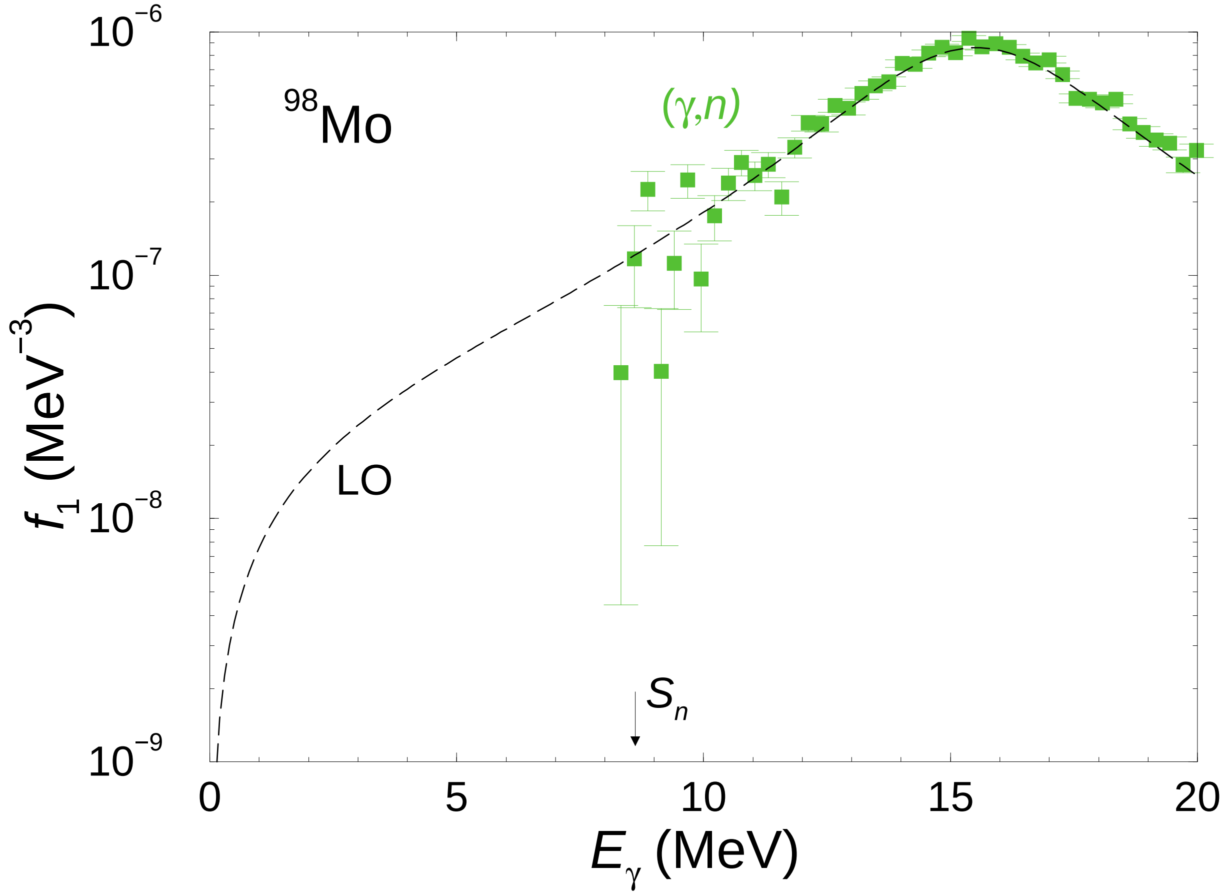

Dipole strength below to the particle-separation energy

- Modelling of astrophysical processes:
  - (γ,n) reaction rates in the p-process.
  - (n,γ) reaction rates in the s-process.
- Studies for future nuclear-fuel cycles:
  - Improved experimental and theoretical description of (n,γ) reactions.
- Open problems:
  - Differences between analytic approximations for dipole strength functions.
  - Discrepancies between strength functions deduced from experiments using different reactions.
  - Influence of nuclear deformation etc. on strength functions.

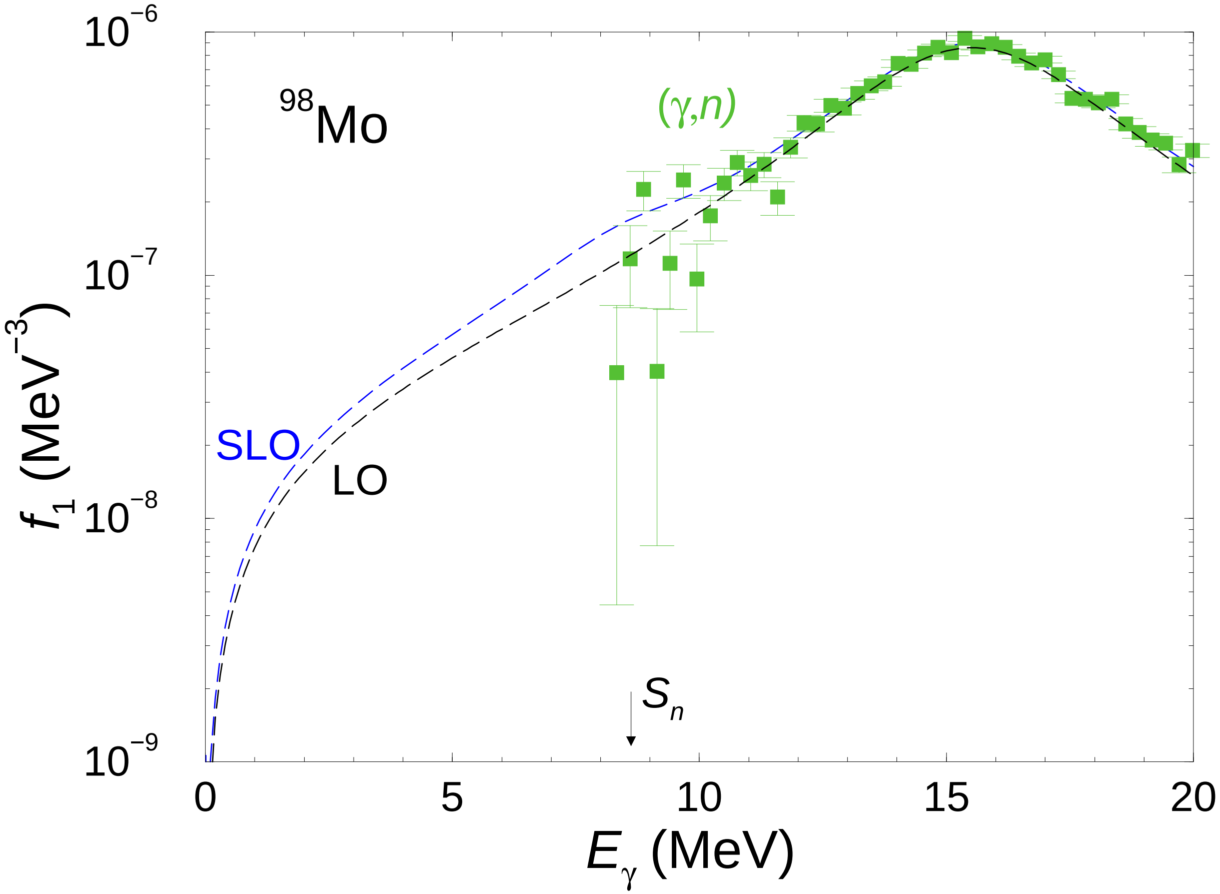

Dipole strength below to the particle-separation energy

- Modelling of astrophysical processes:
  - (γ,n) reaction rates in the p-process.
  - (n,γ) reaction rates in the s-process.
- Studies for future nuclear-fuel cycles:
  - Improved experimental and theoretical description of (n,γ) reactions.
- Open problems:
  - Differences between analytic approximations for dipole strength functions.
  - Discrepancies between strength functions deduced from experiments using different reactions.
  - Influence of nuclear deformation etc. on strength functions.

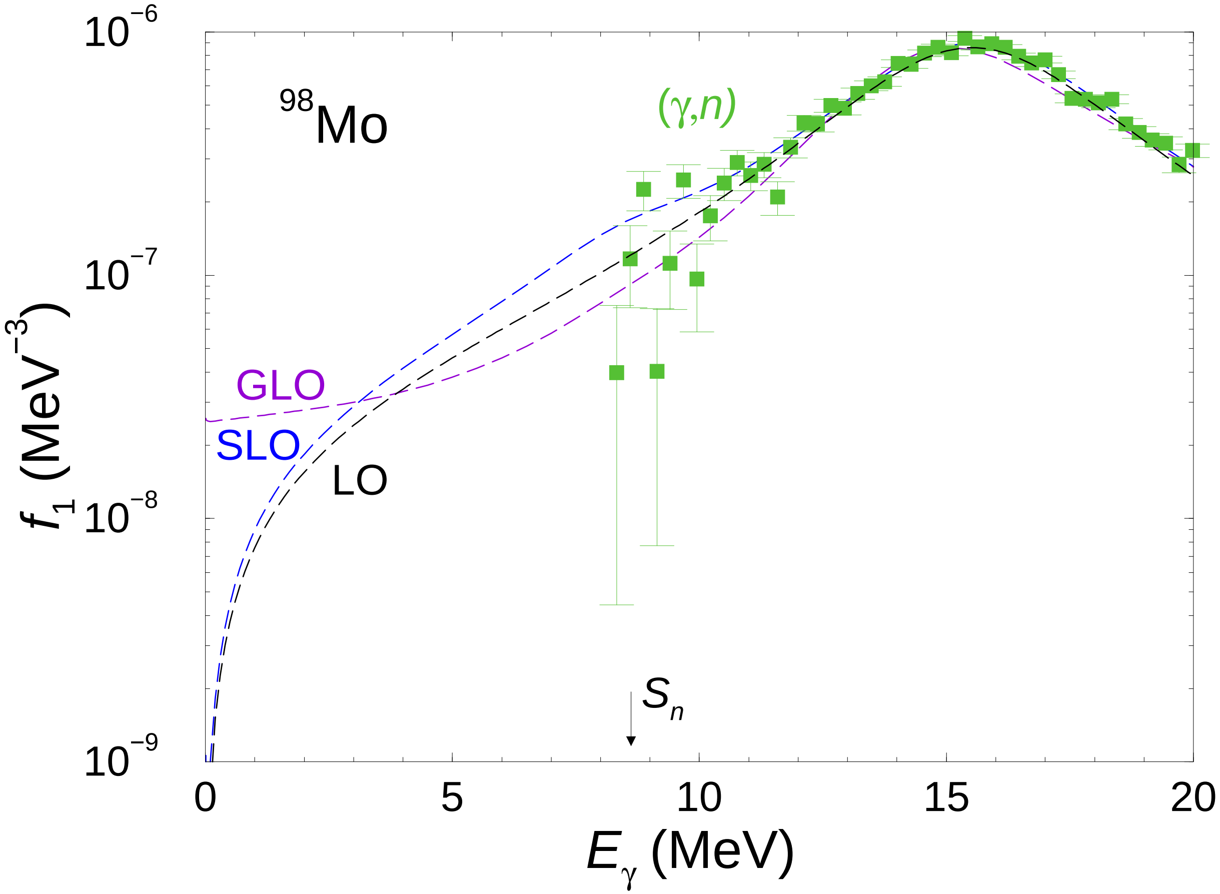

Dipole strength below to the particle-separation energy

- Modelling of astrophysical processes:
  - (γ,n) reaction rates in the p-process.
  - (n,γ) reaction rates in the s-process.
- Studies for future nuclear-fuel cycles:
  - Improved experimental and theoretical description of (n,γ) reactions.
- Open problems:
  - Differences between analytic approximations for dipole strength functions.
  - Discrepancies between strength functions deduced from experiments using different reactions.
  - Influence of nuclear deformation etc. on strength functions.

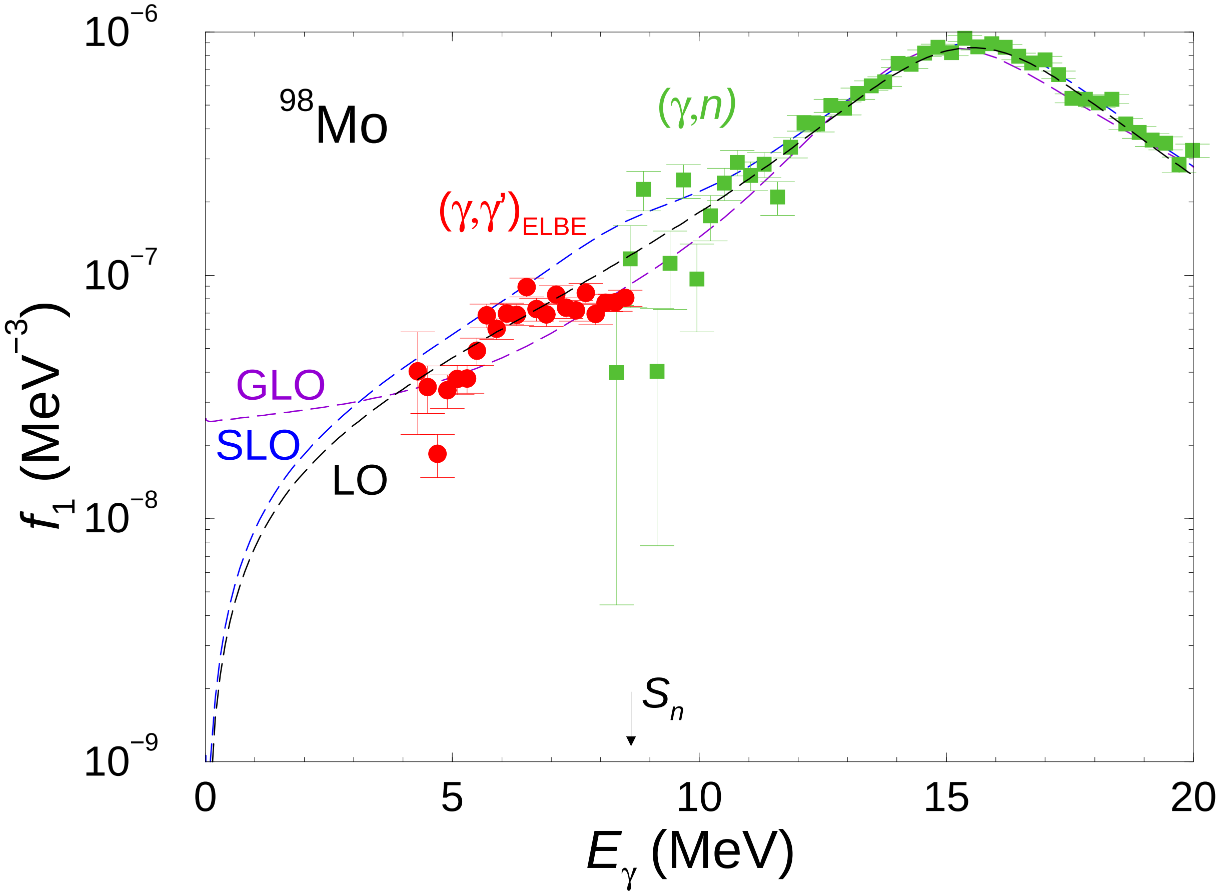

Dipole strength below to the particle-separation energy

- Modelling of astrophysical processes:
  - (γ,n) reaction rates in the p-process.
  - (n,γ) reaction rates in the s-process.
- Studies for future nuclear-fuel cycles:
  - Improved experimental and theoretical description of (n,γ) reactions.
- Open problems:
  - Differences between analytic approximations for dipole strength functions.
  - Discrepancies between strength functions deduced from experiments using different reactions.
  - Influence of nuclear deformation etc. on strength functions.

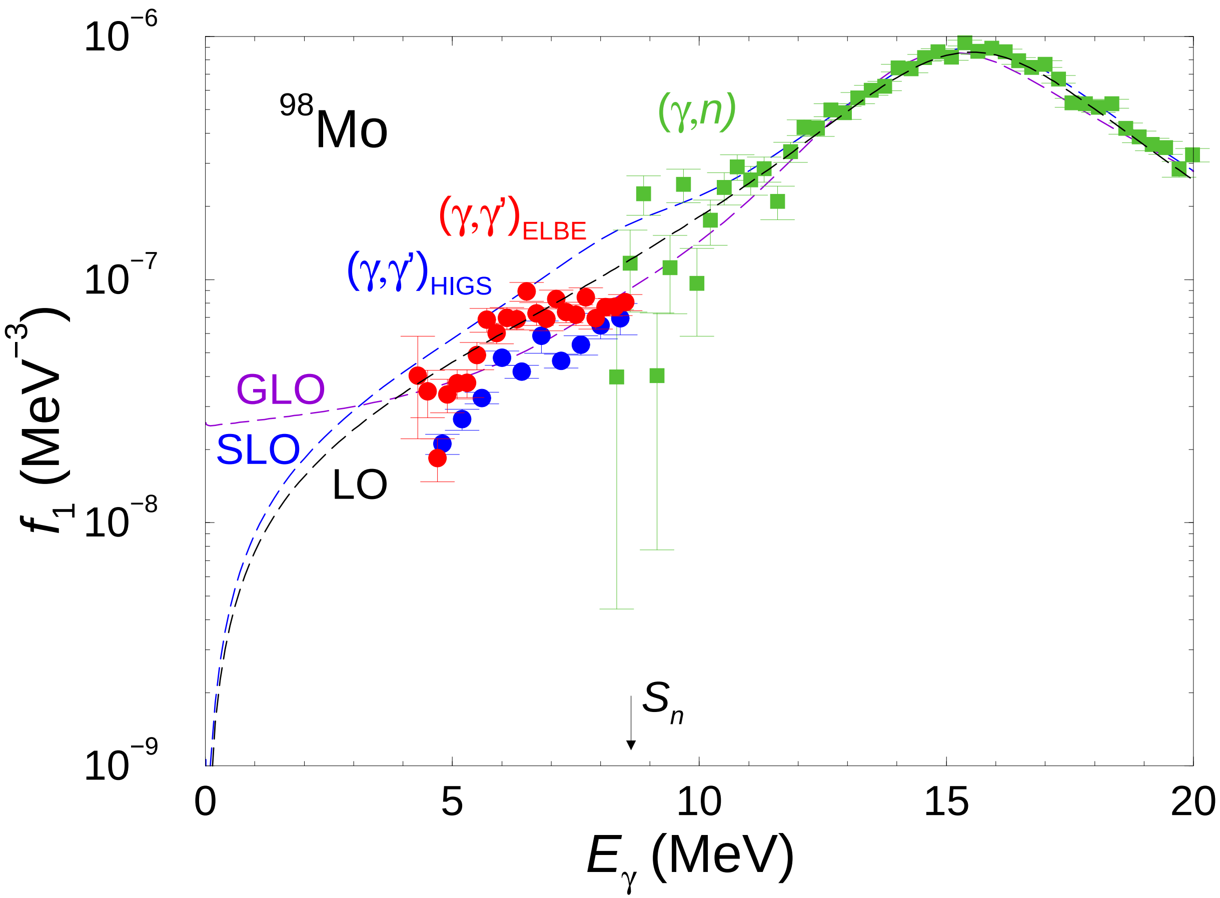

Dipole strength below to the particle-separation energy

- Modelling of astrophysical processes:
  - (γ,n) reaction rates in the p-process.
  - (n,γ) reaction rates in the s-process.
- Studies for future nuclear-fuel cycles:
  - Improved experimental and theoretical description of (n,γ) reactions.
- Open problems:
  - Differences between analytic approximations for dipole strength functions.
  - Discrepancies between strength functions deduced from experiments using different reactions.
  - Influence of nuclear deformation etc. on strength functions.

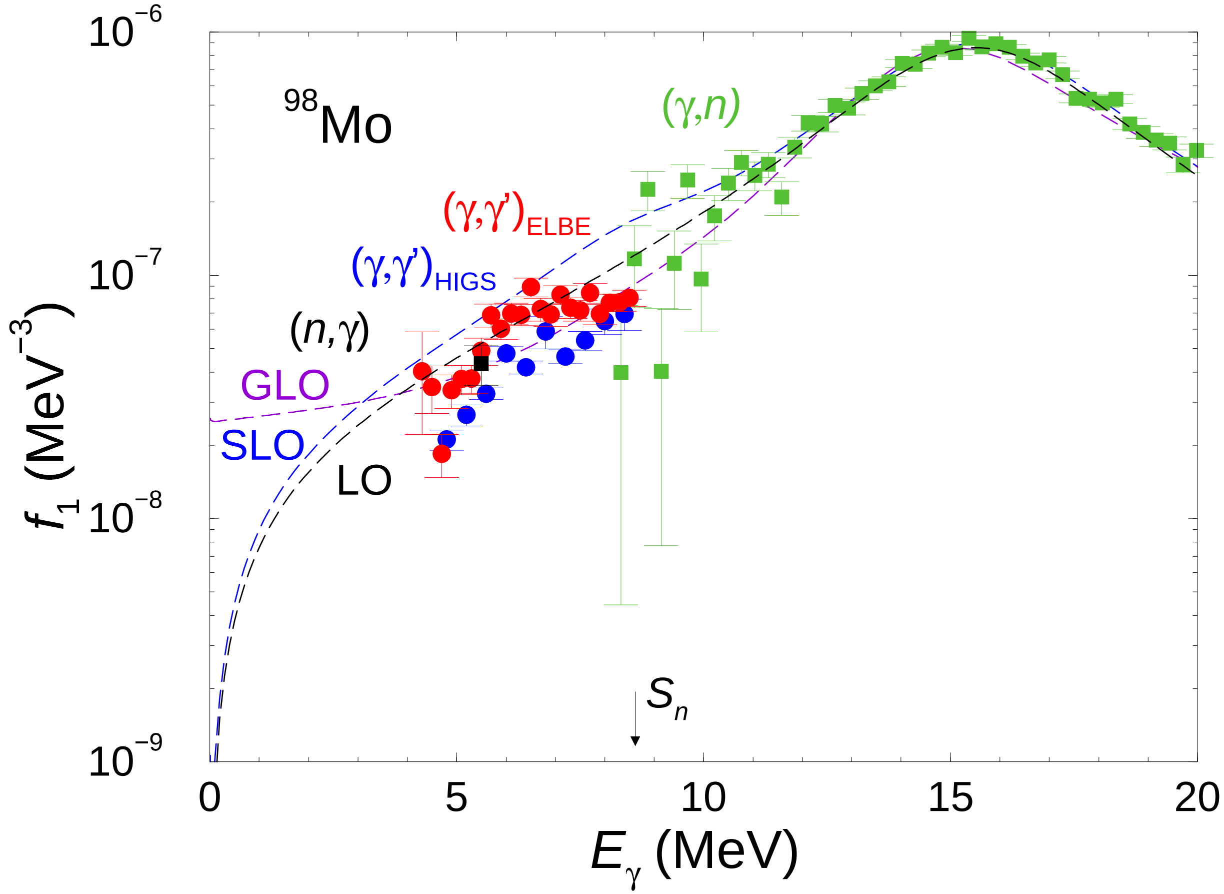

Dipole strength below to the particle-separation energy

- Modelling of astrophysical processes:
  - (γ,n) reaction rates in the p-process.
  - (n,γ) reaction rates in the s-process.
- Studies for future nuclear-fuel cycles:
  - Improved experimental and theoretical description of (n,γ) reactions.
- Open problems:
  - Differences between analytic approximations for dipole strength functions.
  - Discrepancies between strength functions deduced from experiments using different reactions.
  - Influence of nuclear deformation etc. on strength functions.

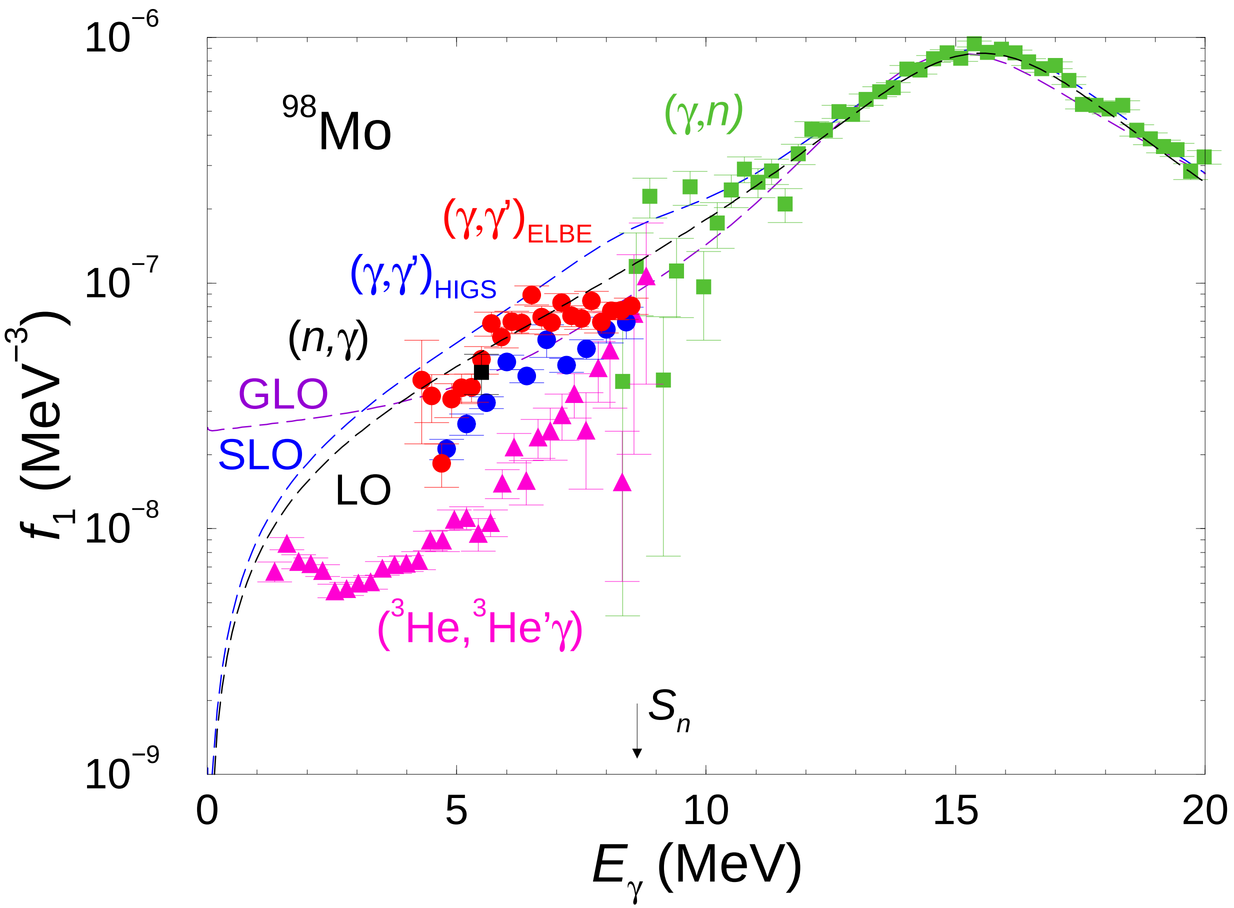

The radiation source ELBE

Electron Linear accelerator of high Brilliance and low Emittance

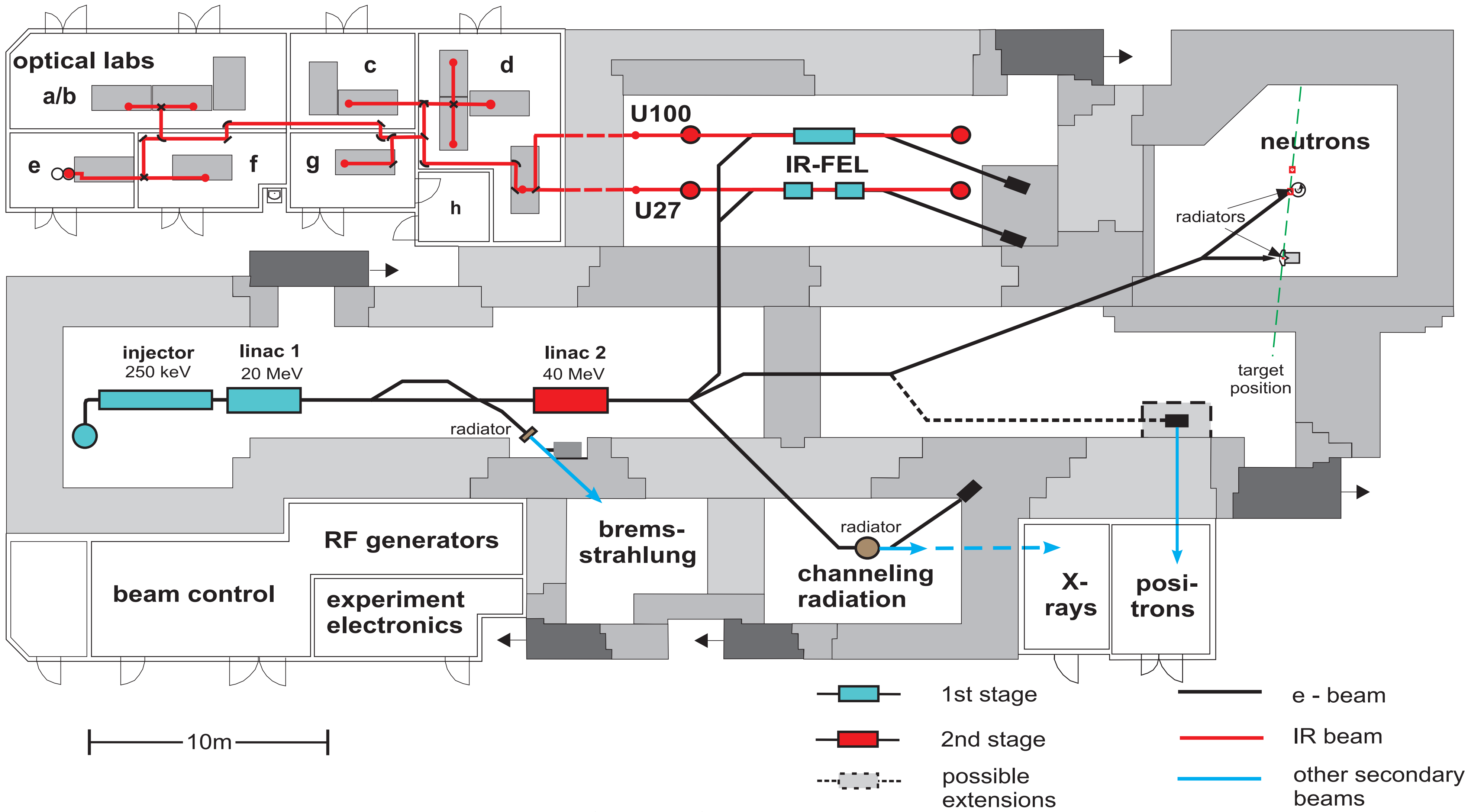

National center for high-power radiation sources at ELBE/HZDR

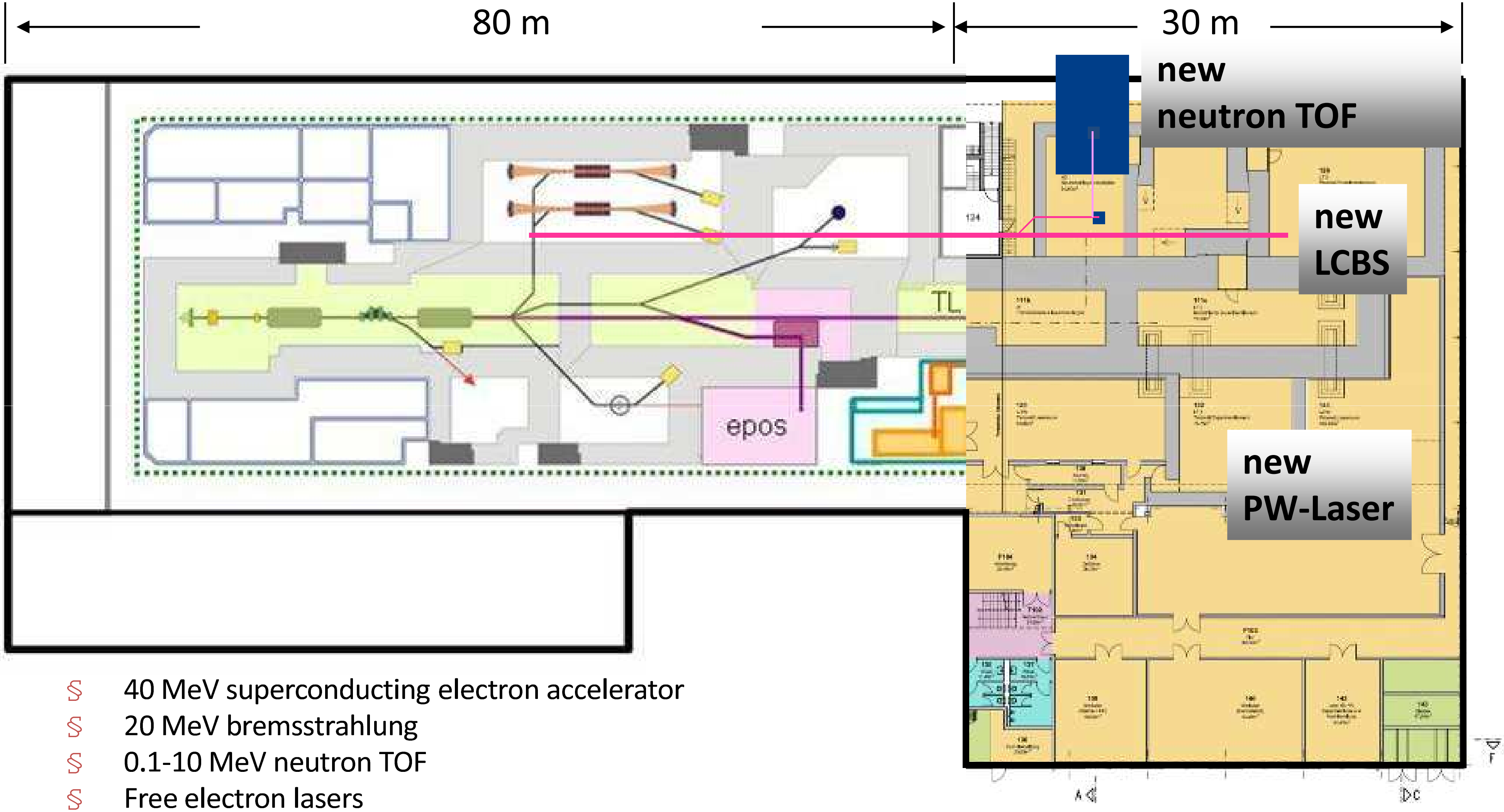

- 40 MeV superconducting electron accelerator
- 20 MeV bremsstrahlung
- 0.1-10 MeV neutron TOF
- Free electron lasers
- X-ray source using Laser-Compton-backscattering
- Petawatt laser for ion acceleration

The bremsstrahlung facility at the electron accelerator ELBE

Accelerator parameters:

- Maximum electron energy: $\approx$ 18 MeV
- Maximum average current: $\approx$ 0.8 mA
- Micro-pulse rate: 13 MHz
- Micro-pulse length: $\approx$ 5 ps

R.S. et al., NIM A 555, 211 (2005)

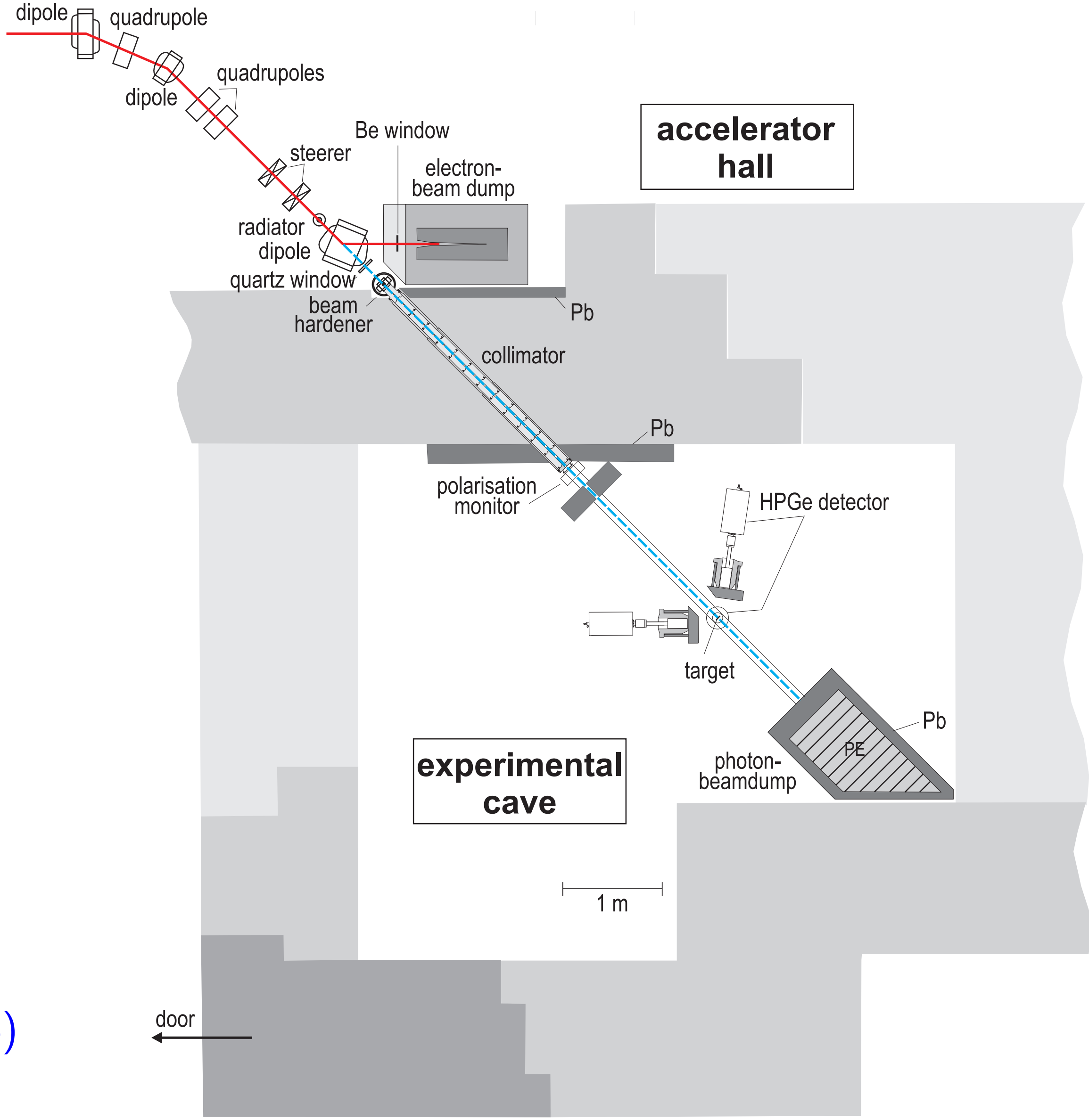

Detector setup

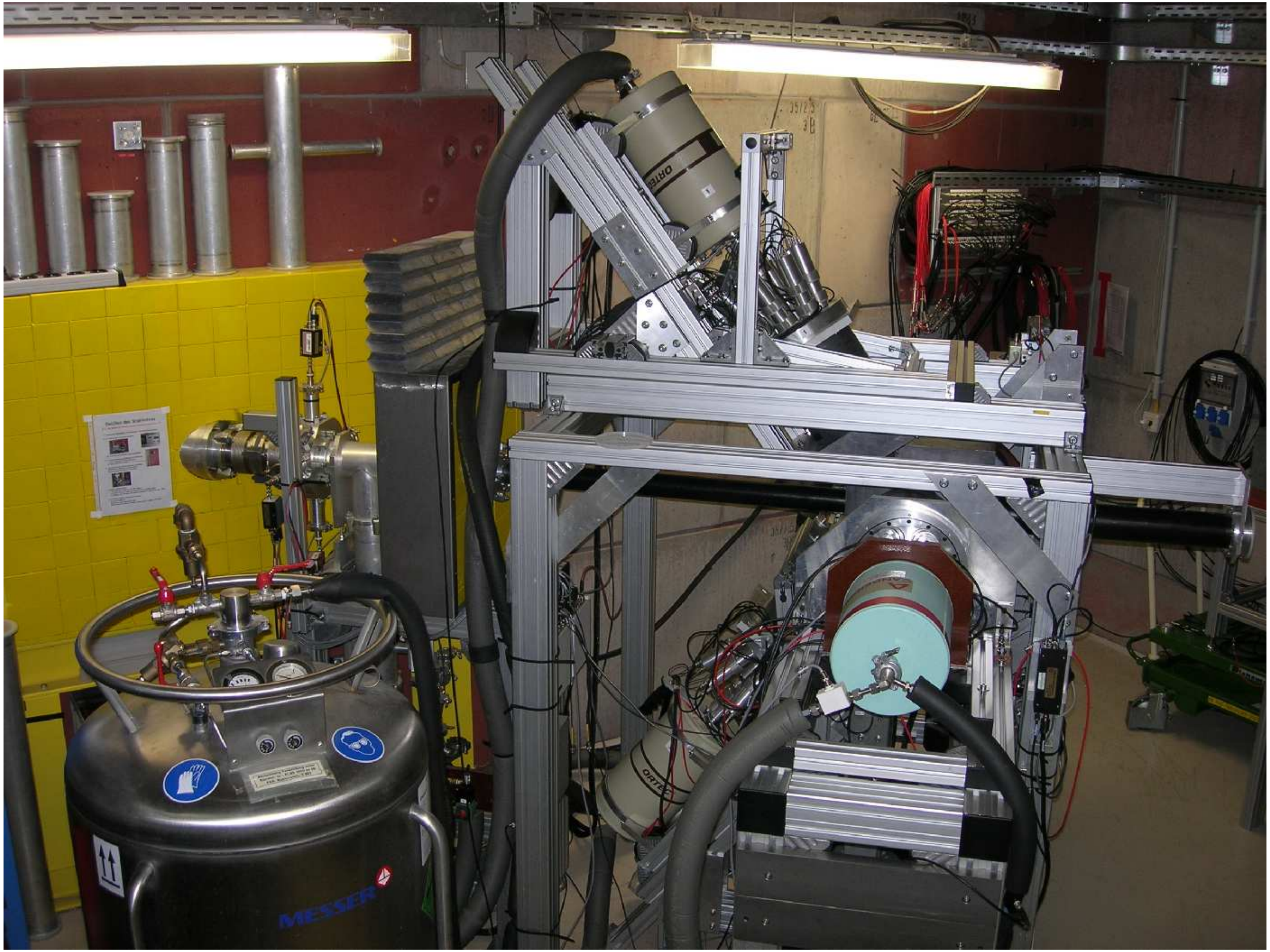

Problem of feeding and branching

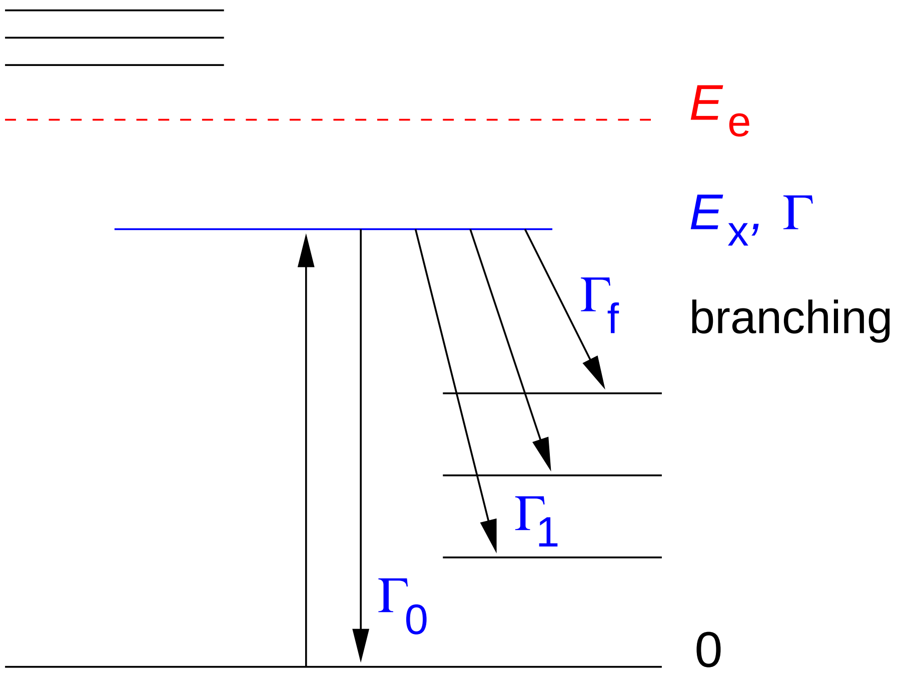

Measured intensity of a γ transition:

$$I_\gamma(E_\gamma, \Theta) = I_s(E_x)\, \Phi_\gamma(E_x)\, \epsilon(E_\gamma)\, N_{at}\, W(\Theta)\, \Delta\Omega$$

Integrated scattering cross section:

$$I_s = \int \sigma_{\gamma\gamma}\, dE = \frac{2J_x+1}{2J_0+1}\left(\frac{\pi\hbar c}{E_x}\right)^2 \frac{\Gamma_0}{\Gamma}\, \Gamma_0$$

Absorption cross section:

$$\sigma_\gamma = \sigma_{\gamma\gamma}\left(\frac{\Gamma_0}{\Gamma}\right)^{-1}$$

E1 strength:

$$B(E1) \sim \Gamma_0 / E_\gamma^3$$

Problem of feeding and branching

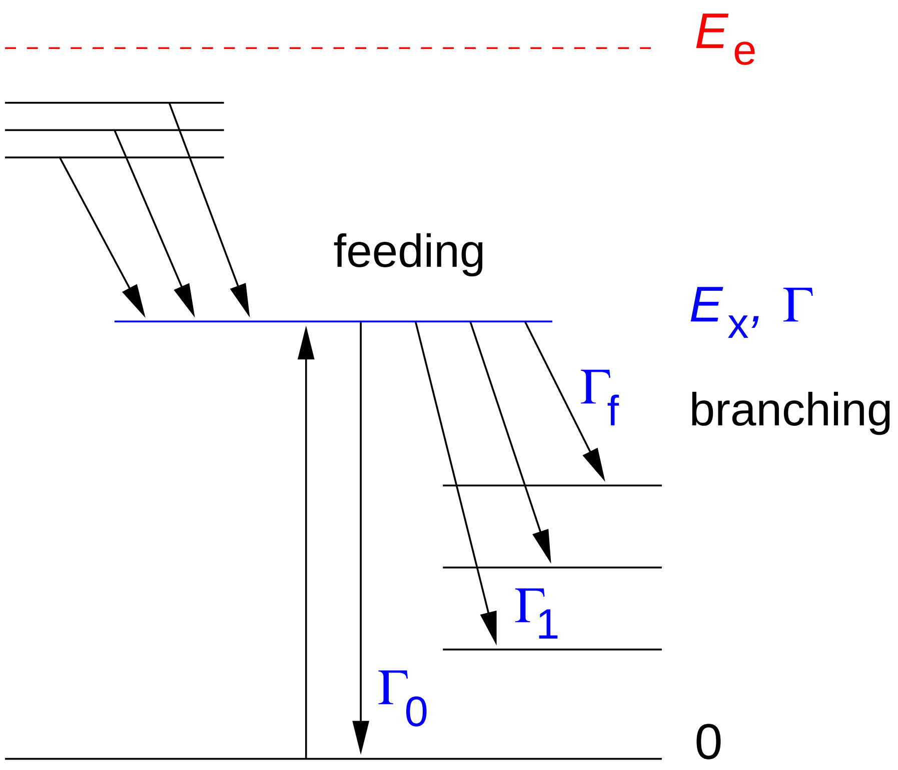

Measured intensity of a γ transition:

$$I_\gamma(E_\gamma, \Theta) > I_s(E_x)\, \Phi_\gamma(E_x)\, \epsilon(E_\gamma)\, N_{at}\, W(\Theta)\, \Delta\Omega$$

Integrated scattering cross section:

$$I_s = \int \sigma_{\gamma\gamma}\, dE = \frac{2J_x+1}{2J_0+1} \left(\frac{\pi\hbar c}{E_x}\right)^2 \frac{\Gamma_0}{\Gamma}\, \Gamma_0$$

Absorption cross section:

$$\sigma_\gamma = \sigma_{\gamma\gamma} \left(\frac{\Gamma_0}{\Gamma}\right)^{-1}$$

E1 strength:

$$B(E1) \sim \Gamma_0 / E_\gamma^3$$

Unresolved strength in the continuum

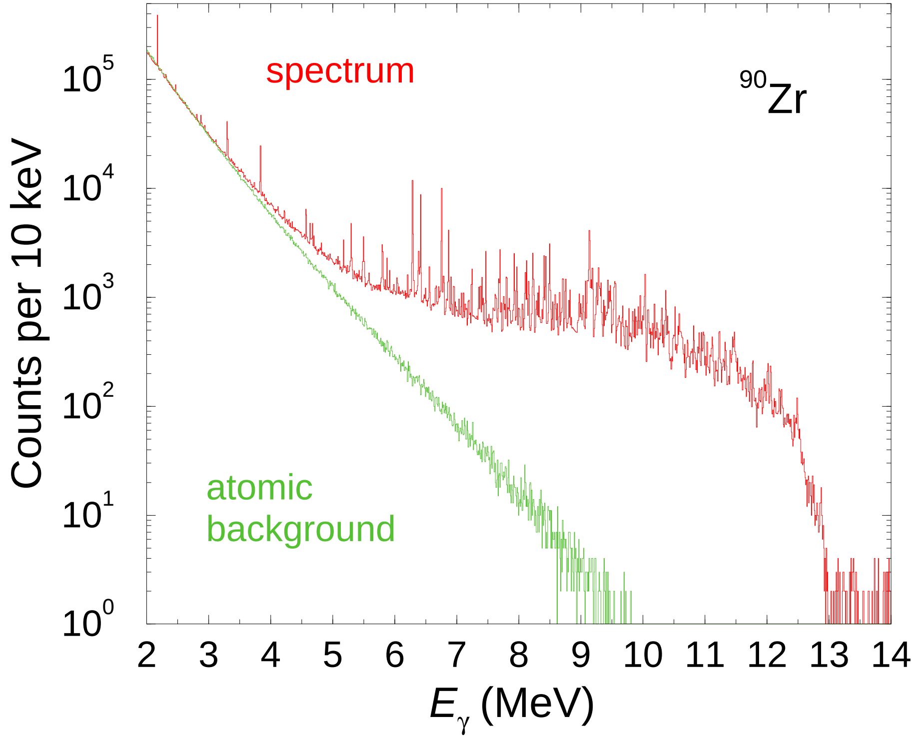

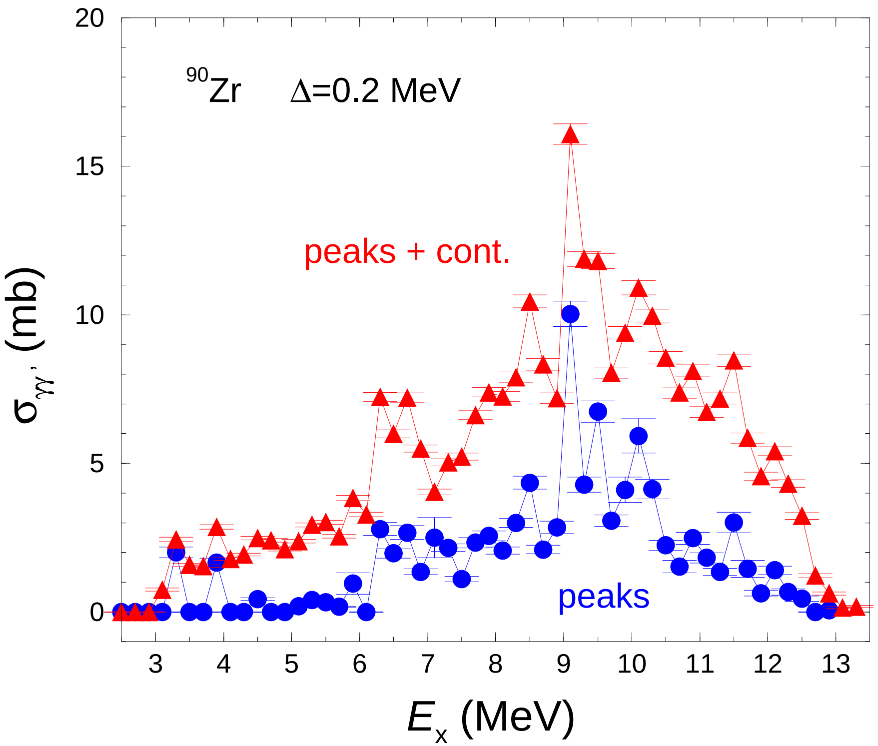

Experimental spectrum of ^{90}Zr (corrected for room background, detector response, efficiency, measuring time) and simulated spectrum of atomic background.

Scattering cross sections in ^{90}Zr averaged over energy bins of 0.2 MeV, not corrected for branching, derived from the difference of the experimental spectrum and the atomic background (triangles) and from the resolved peaks only (circles).

Unresolved strength in the continuum

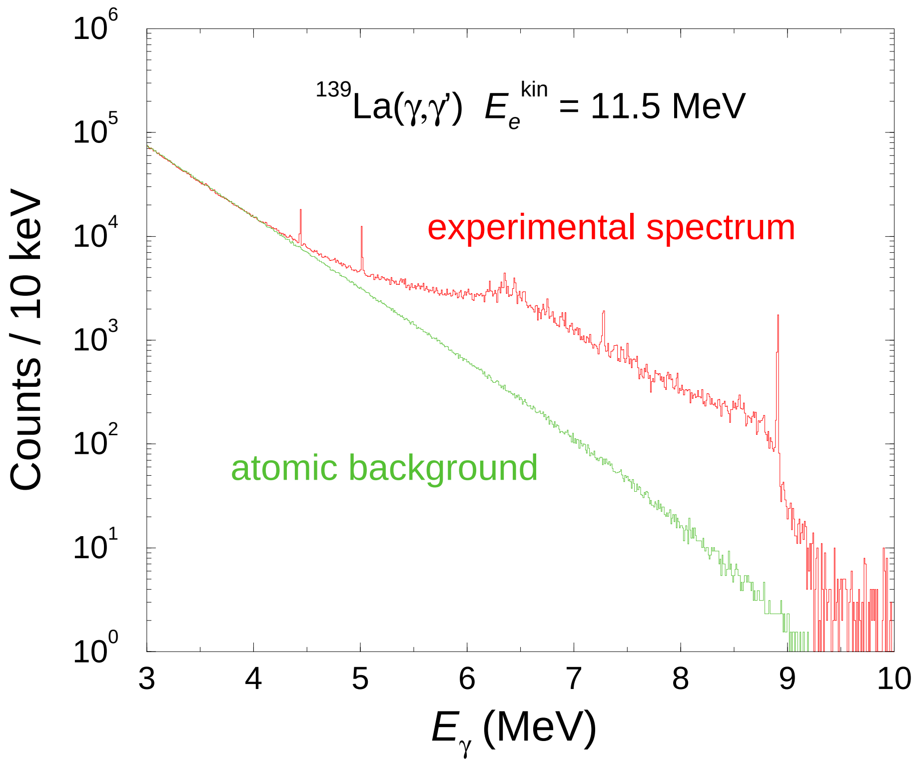

Experimental spectrum of ^{139}La (corrected for room background, detector response, efficiency, measuring time) and simulated spectrum of atomic background.

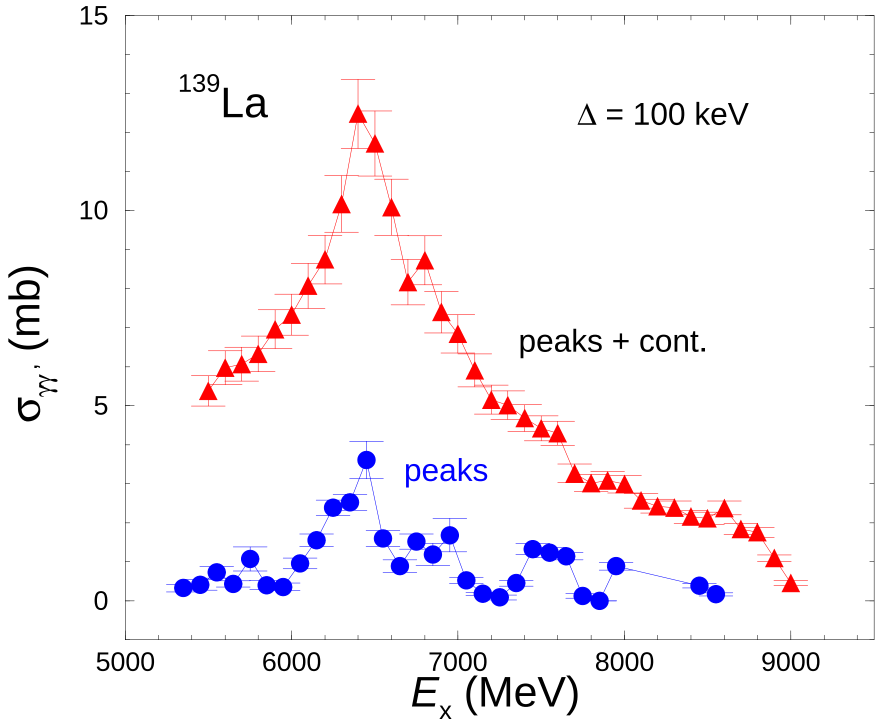

Scattering cross sections in ^{139}La averaged over energy bins of 0.1 MeV, not corrected for branching, derived from the difference of the experimental spectrum and the atomic background (triangles) and from the resolved peaks only (circles).

Simulations of γ-ray cascades

Monte Carlo simulations of γ-ray cascades from groups of levels in 100 keV bins (G. Rusev, dissertation)

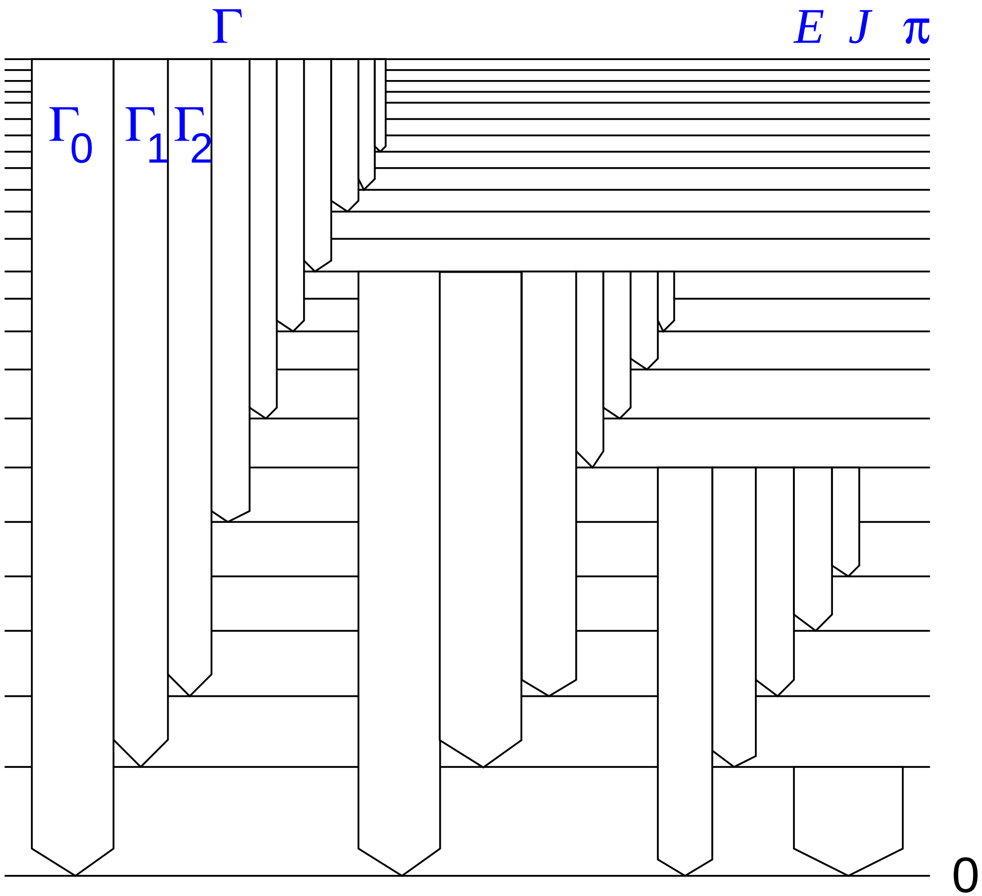

⇒ Level scheme of $J = |J_0 \pm 1, 2|$ states constructed by using:

∘ Backshifted Fermi-Gas Model with level-density parameters from T. v. Egidy, D. Bucurescu, PRC 80, 054310 (2009)

∘ Wigner level-spacing distributions

⇒ Partial decay widths calculated by using:

∘ Photon strength functions approximated by Lorentz curves (www-nds.iaea.org/RIPL-2).
$E1$: parameters from fit to (γ,n) data
$M1$: global parametrisation of spin-flip resonances
$E2$: global parametrisation of isoscalar resonances

∘ Porter-Thomas distributions of decay widths.

⇒ Feeding intensities subtracted and intensities of g.s. transitions corrected with calculated branching ratios Γ_0/Γ.

Simulations of γ-ray cascades

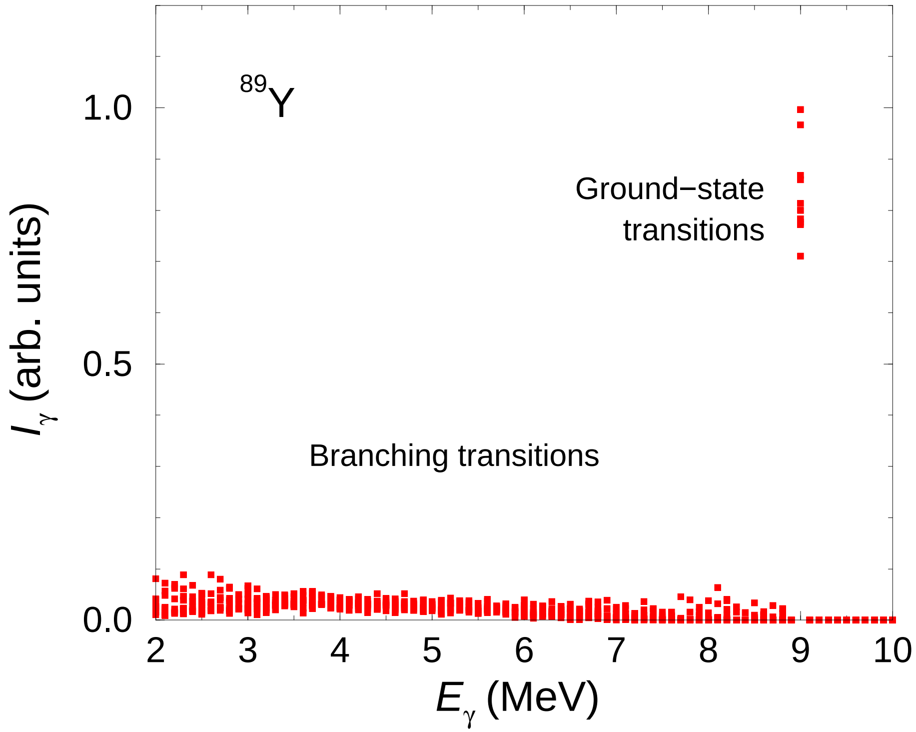

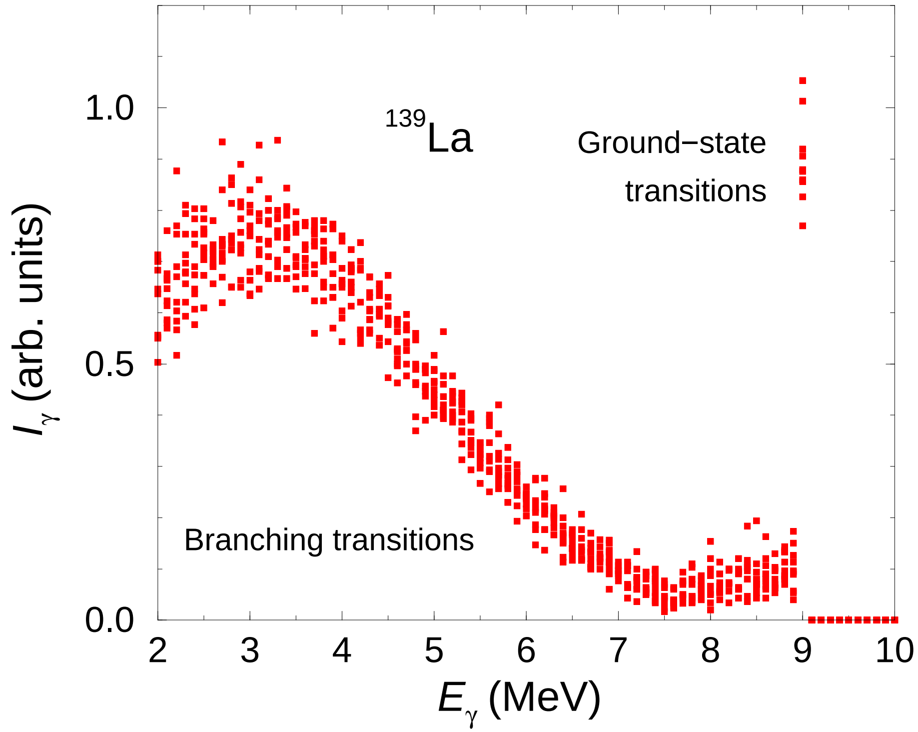

Simulated intensity distribution of transitions depopulating levels in a 100 keV bin around 9 MeV.

$\Rightarrow$ Subtraction of intensities of branching transitions.

^{89}Y data: N. Benouaret et al., PRC 79, 014303 (2009).

^{139}La data: A. Makinaga et al., PRC 82, 024314 (2010).

Simulations of γ-ray cascades

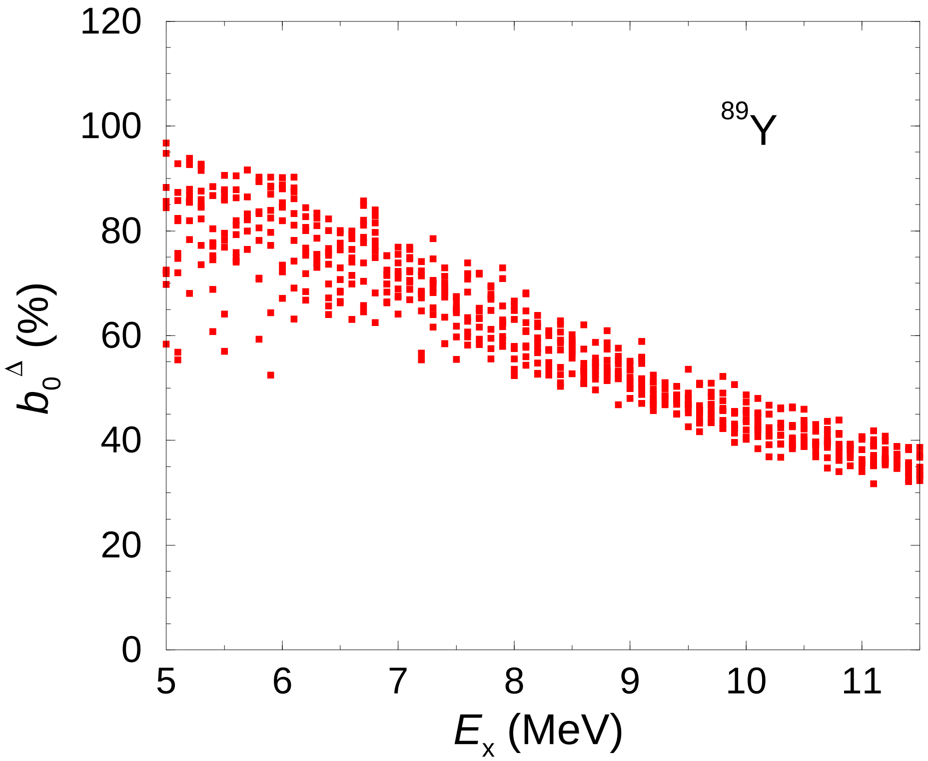

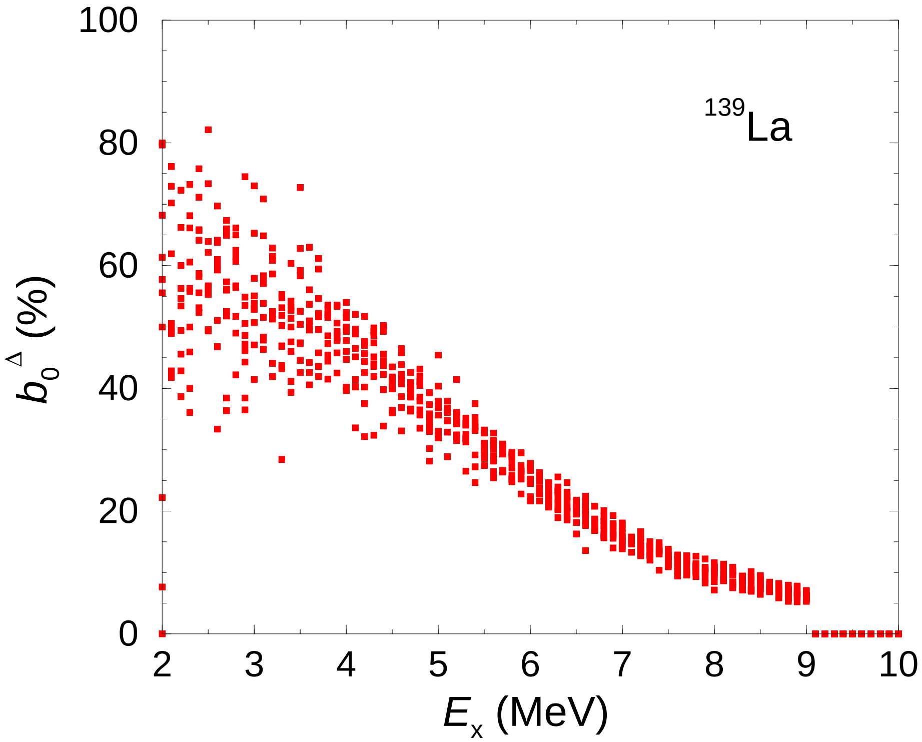

Distribution of branching ratios $b_0 = \Gamma_0/\Gamma$ versus the excitation energy as obtained from the simulations of γ-ray cascades.

$\Rightarrow$ Estimate of Γ_0 and σ_γ.

^{89}Y data: N. Benouaret et al., PRC 79, 014303 (2009).
^{139}La data: A. Makinaga et al., PRC 82, 024314 (2010).

Absorption cross section of ^{139}La

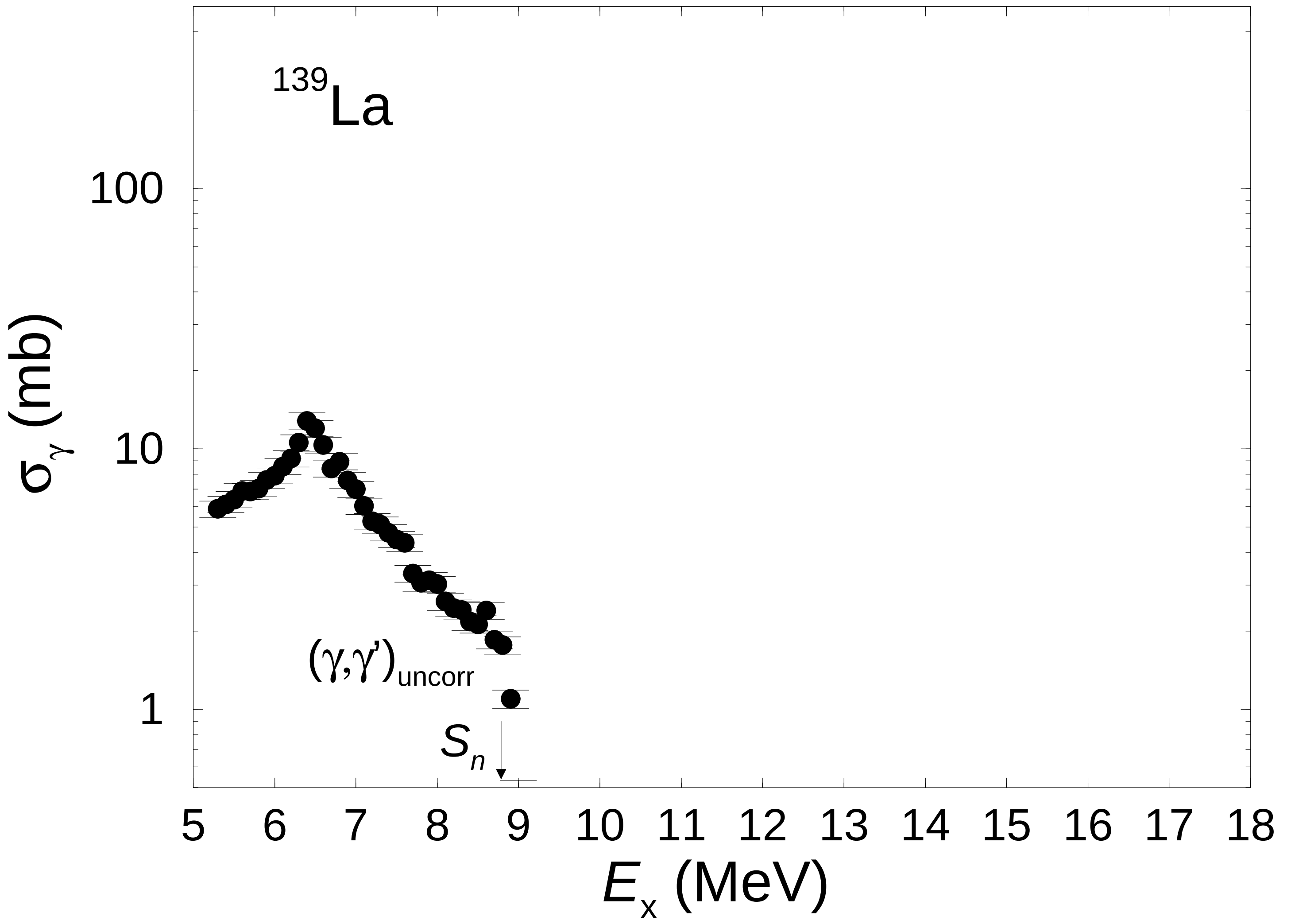

Present (γ, γ) data

Absorption cross section of ^{139}La

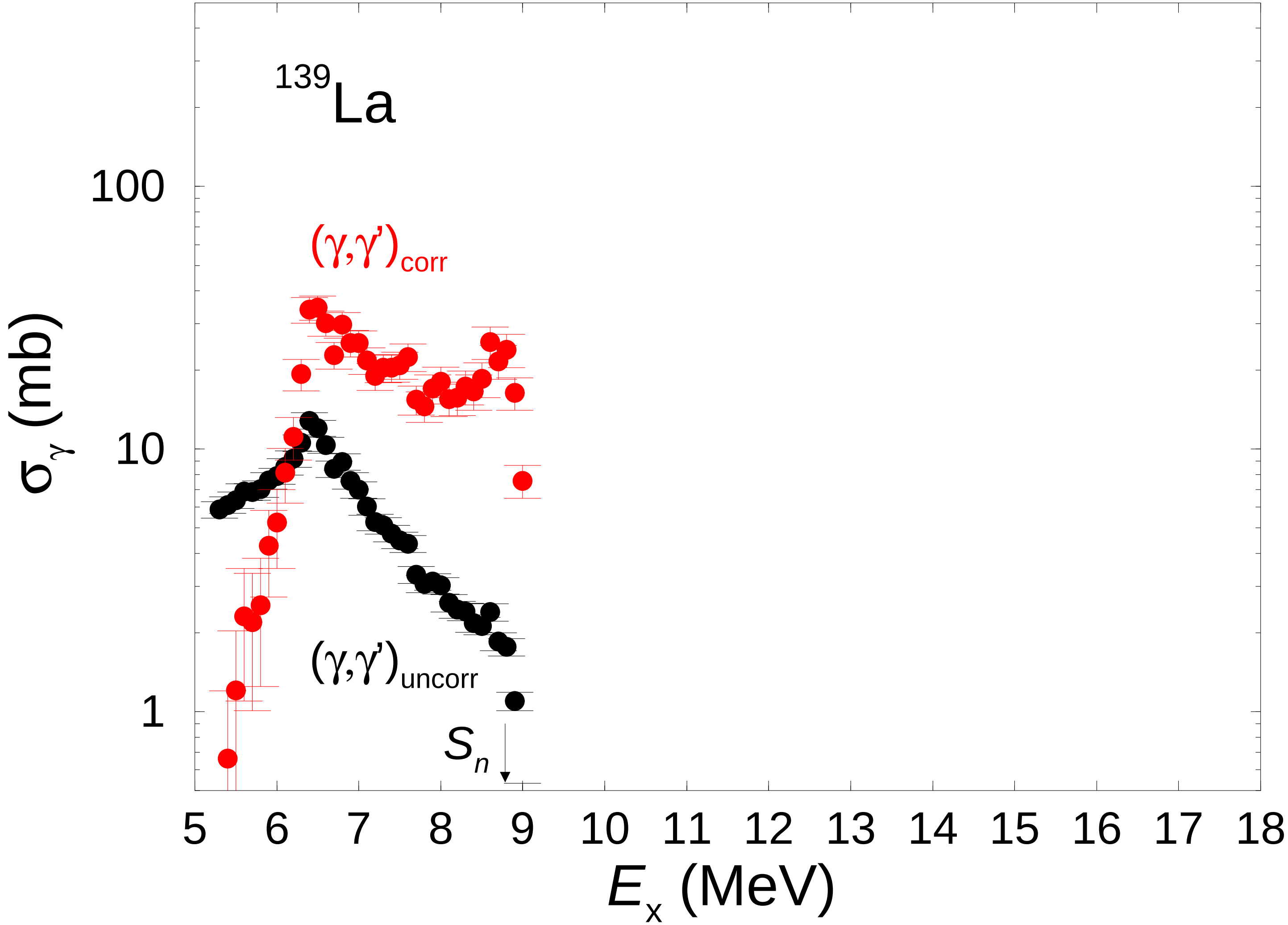

Present (γ, γ) data

Corrected (γ, γ) data

Absorption cross section of ^{139}La

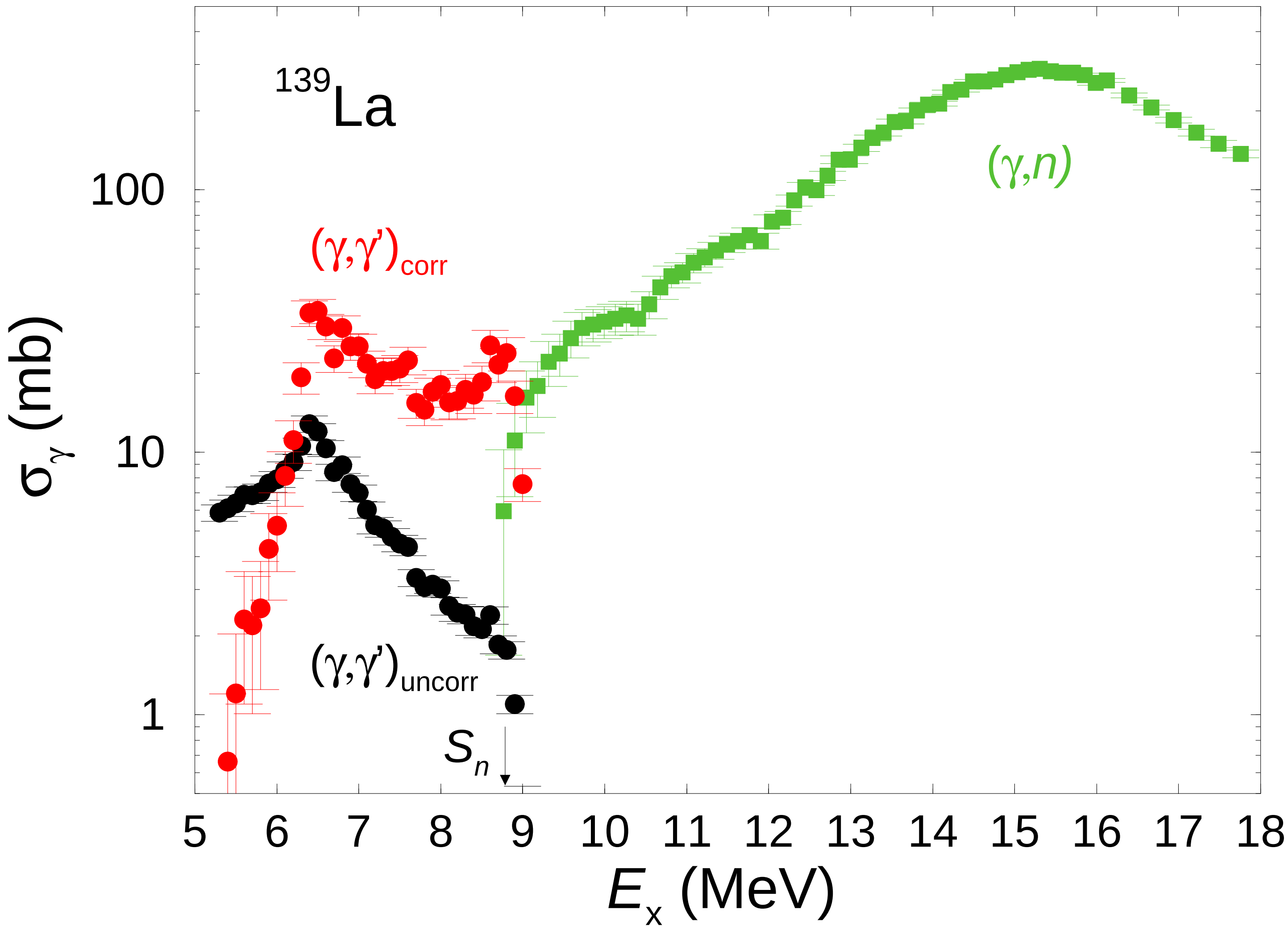

Present (γ,γ) data

Corrected (γ,γ) data

(γ,n) data $(\times\ 0.85)$
NPA 175, 609 (1971)

Absorption cross section of ^{139}La

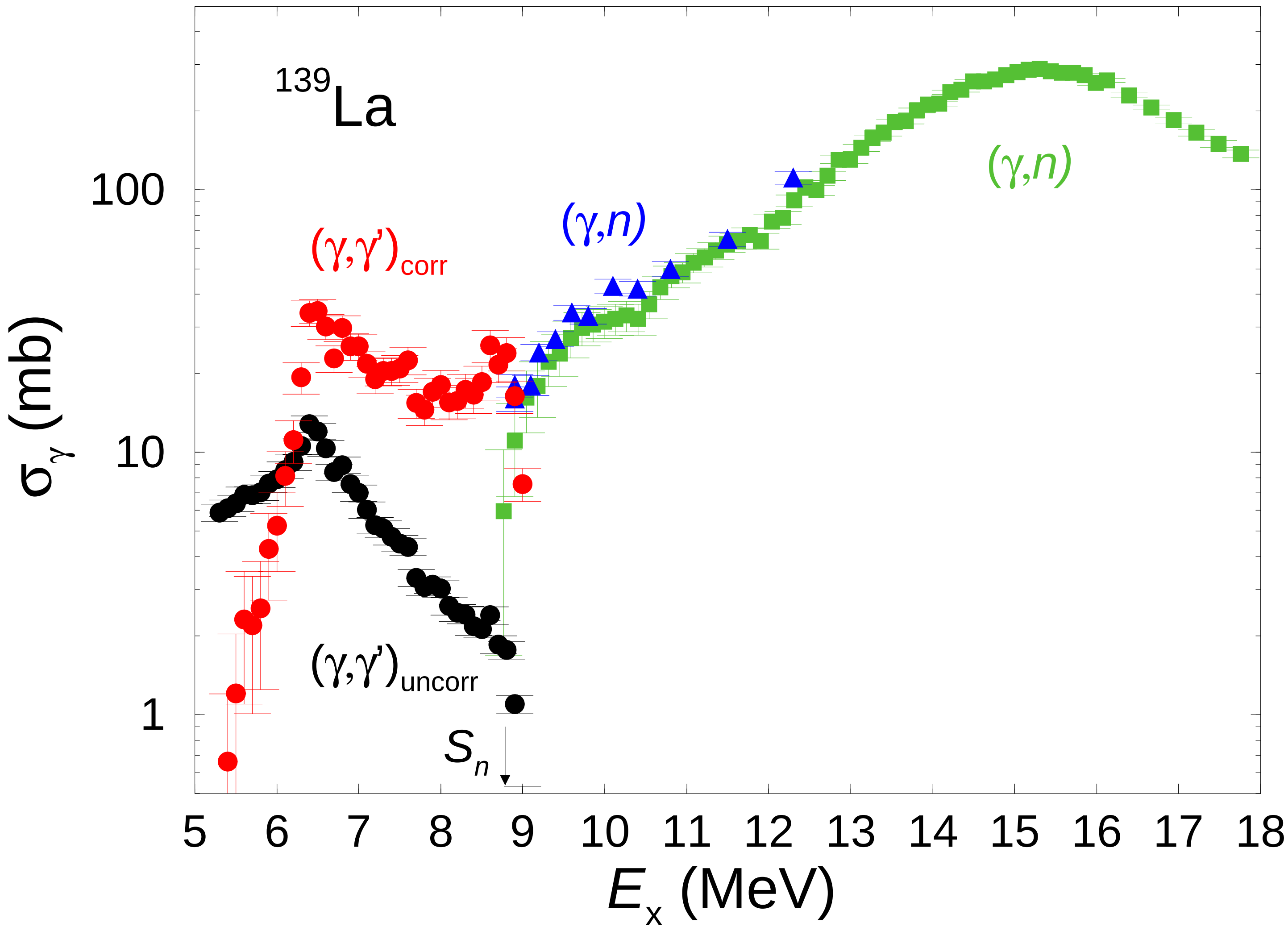

Present (γ, γ) data

Corrected (γ, γ) data

(γ, n) data $(\times\ 0.85)$
NPA 175, 609 (1971)

(γ, n) data
PRC 74, 025806 (2006)

Absorption cross section in ^{139}La

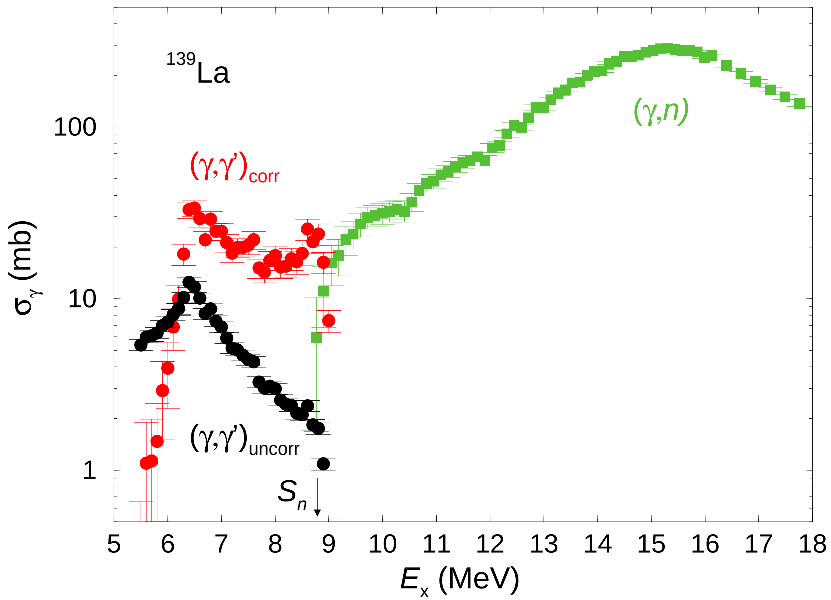

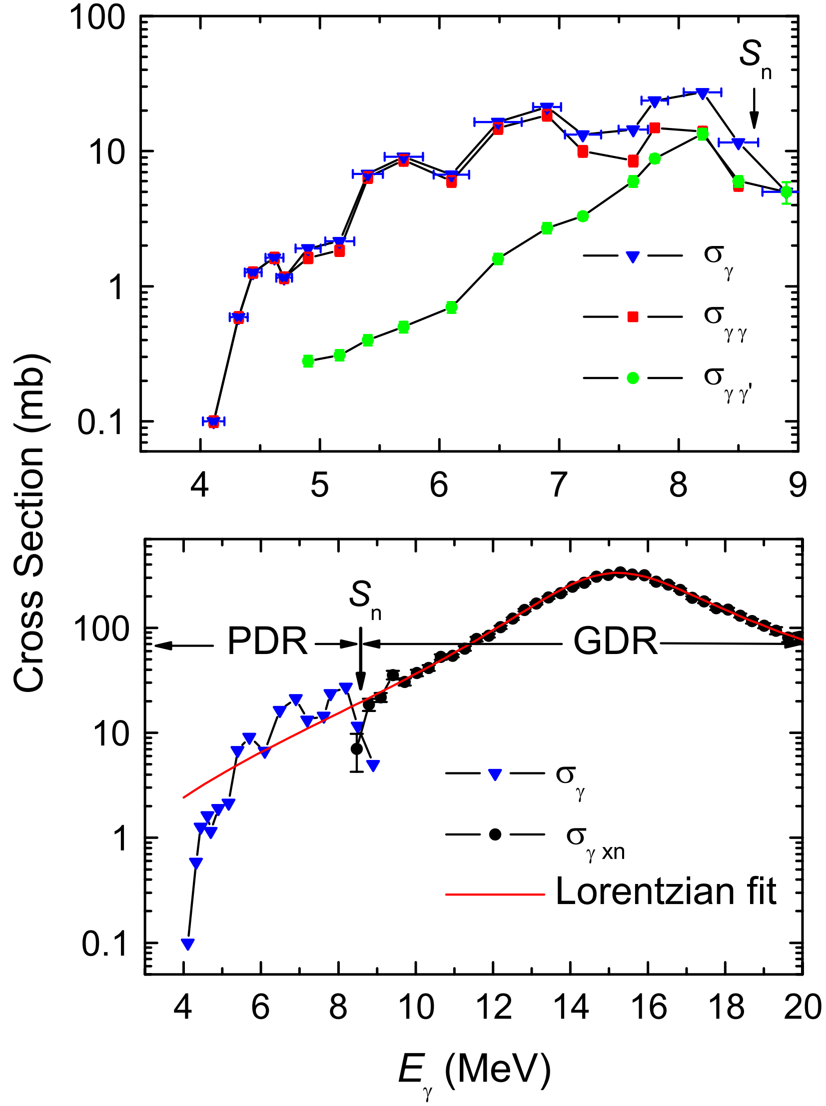

Present data for ^{139}La
A. Makinaga et al., PRC 82, 024314 (2010)

HIGS data for ^{138}Ba
A. Tonchev et al., PRL 104, 072501 (2010)

Absorption cross section of ^{139}La

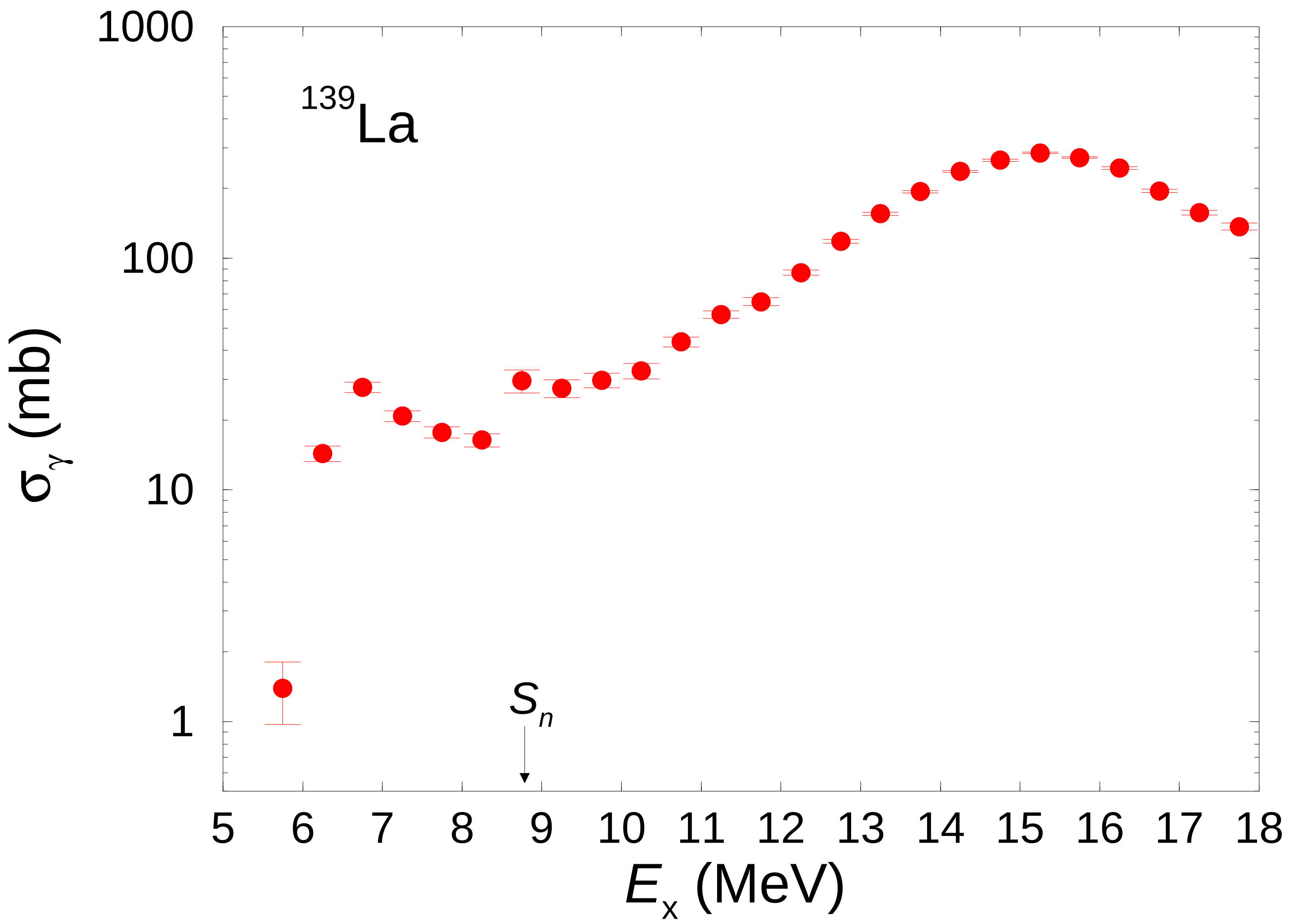

Present (γ, γ) data
$+$ (γ, n) data

Absorption cross section of ^{139}La

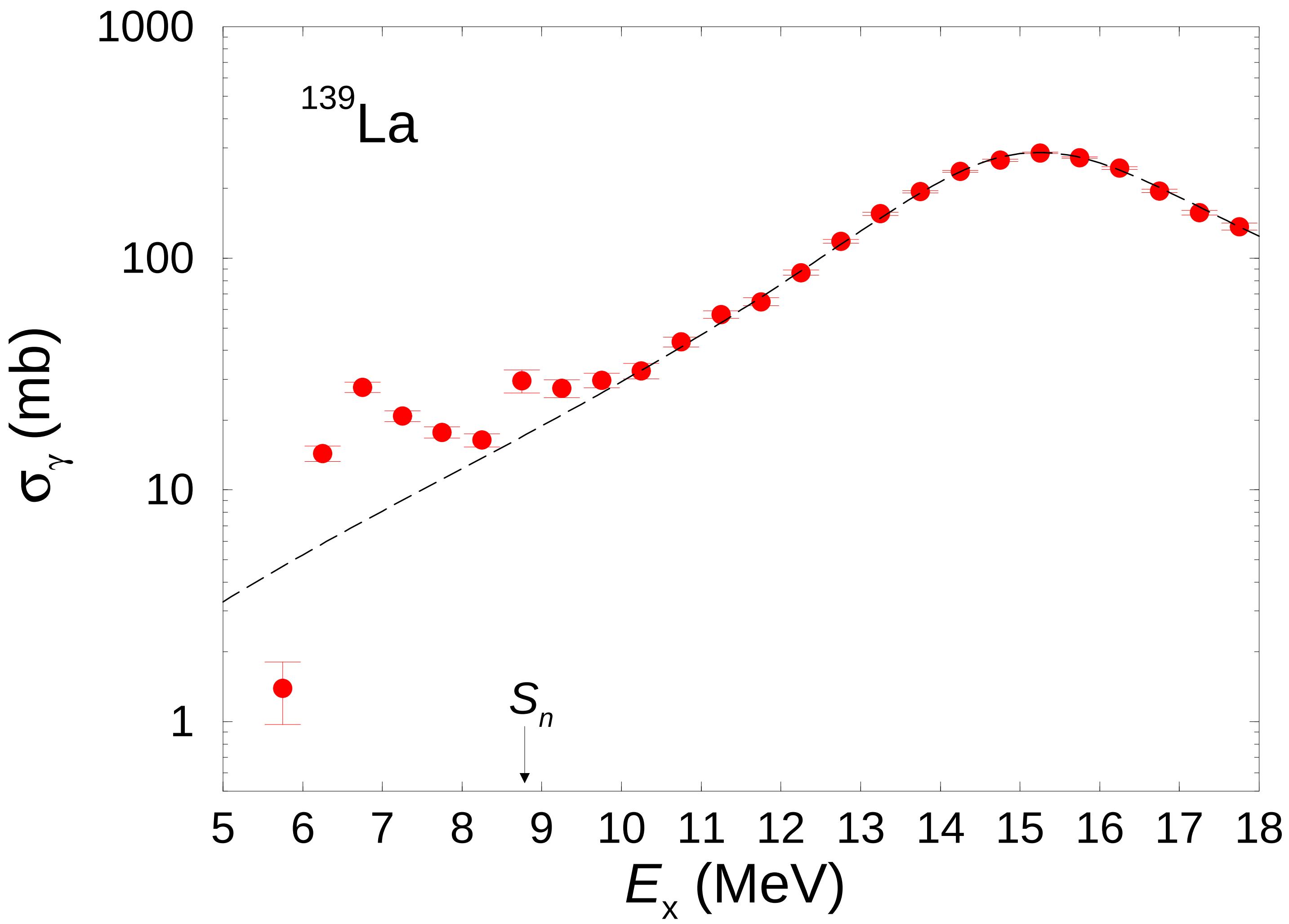

Present (γ, γ) data
$+ (\gamma, n)$ data

Lorentz curve:

$E_0 = 15.24$ MeV

$\Gamma = 4.47$ MeV

$\frac{\pi}{2}\sigma_0\Gamma = 60 \frac{NZ}{A}$ MeV mb

Absorption cross section of ^{139}La

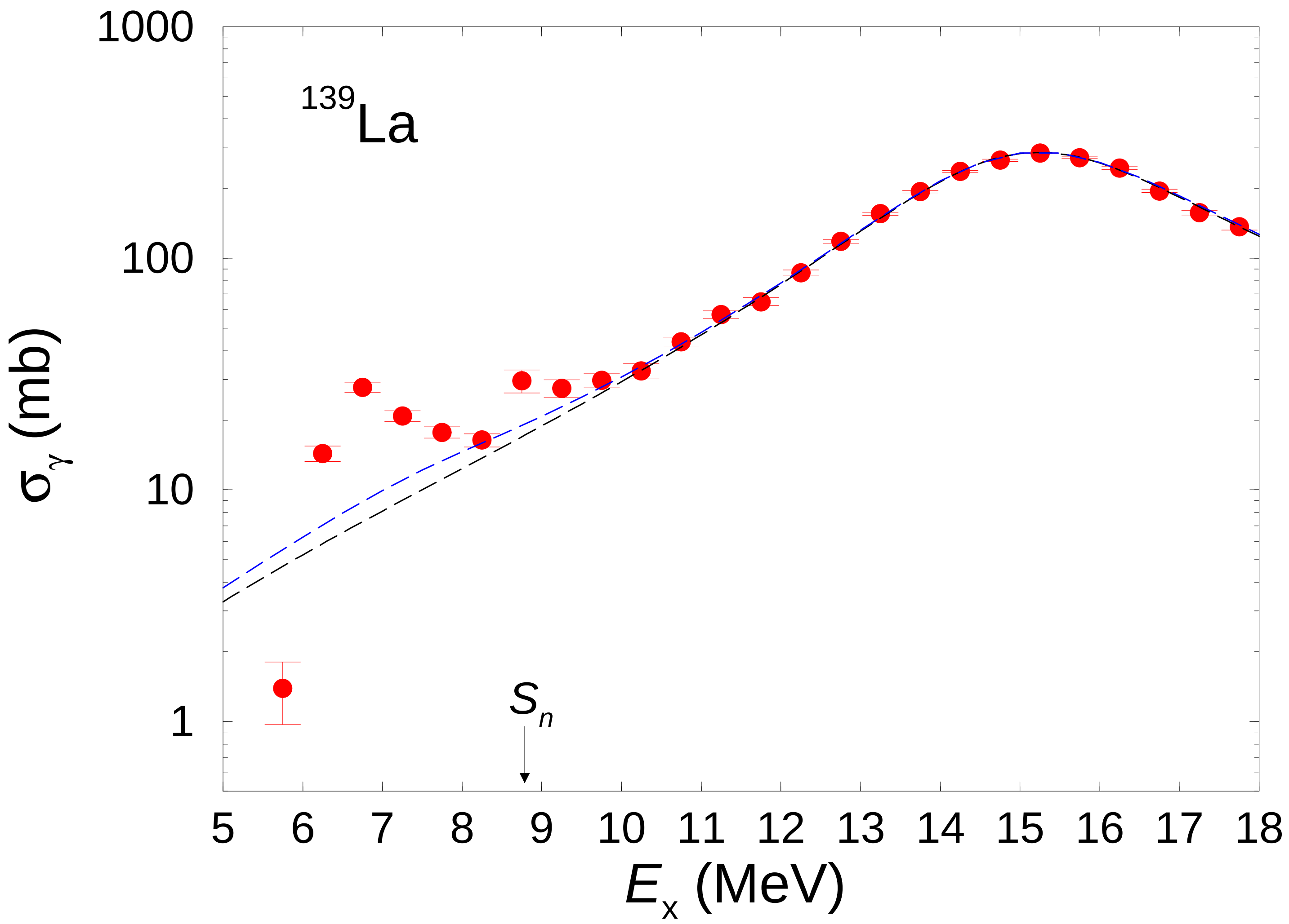

Present (γ, γ) data
$+ (\gamma, n)$ data

Lorentz curve:

$E_0 = 15.24$ MeV

$\Gamma = 4.47$ MeV

$\frac{\pi}{2}\sigma_0\Gamma = 60 \frac{NZ}{A}$ MeV mb

SLO + M1

Absorption cross section of ^{139}La

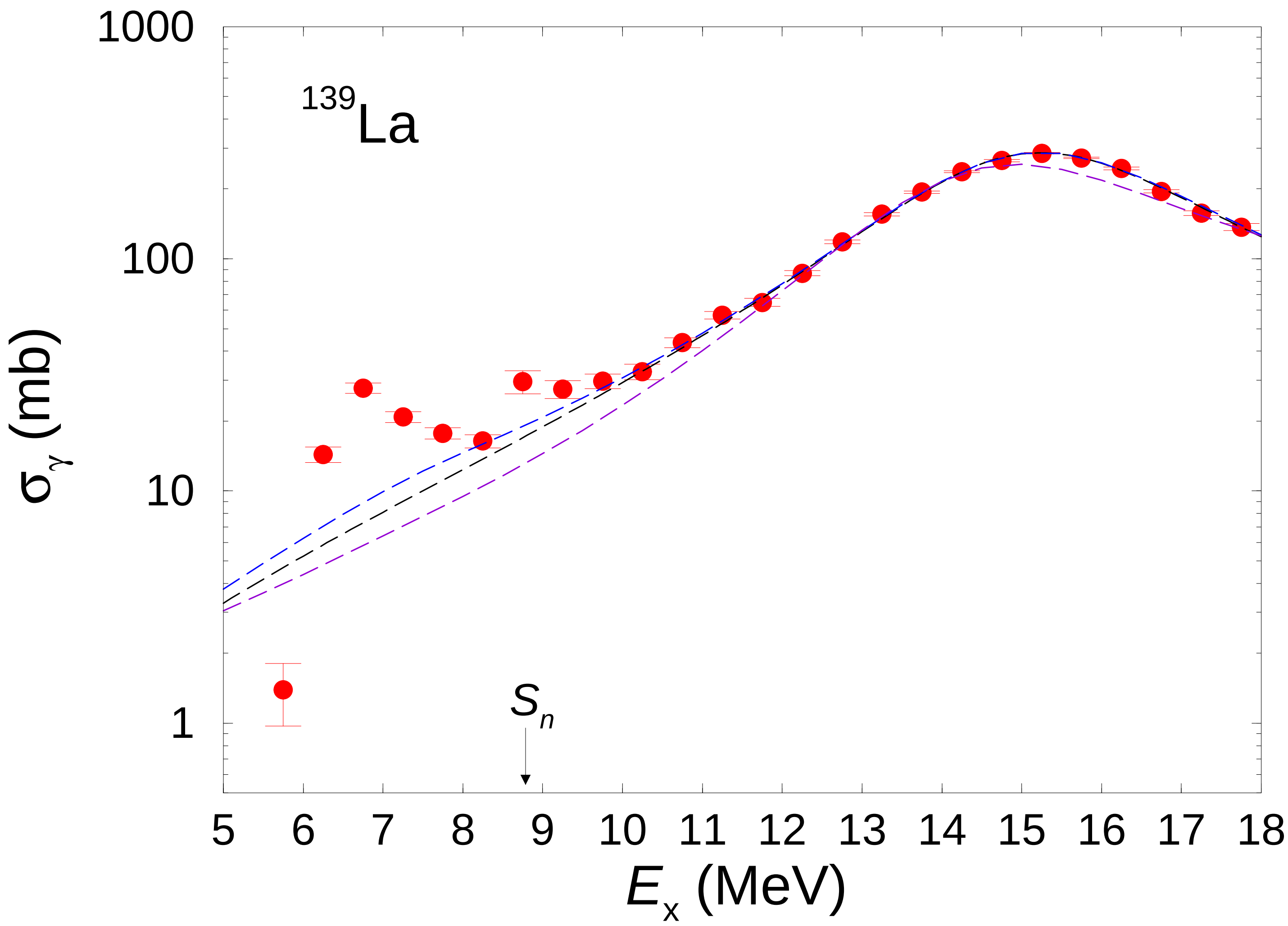

Present (γ,γ) data
$+ (\gamma, n)$ data

Lorentz curve:

$E_0 = 15.24$ MeV

$\Gamma = 4.47$ MeV

$\frac{\pi}{2}\sigma_0\Gamma = 60 \frac{NZ}{A}$ MeV mb

SLO + M1

GLO + M1

Absorption cross section of ^{139}La

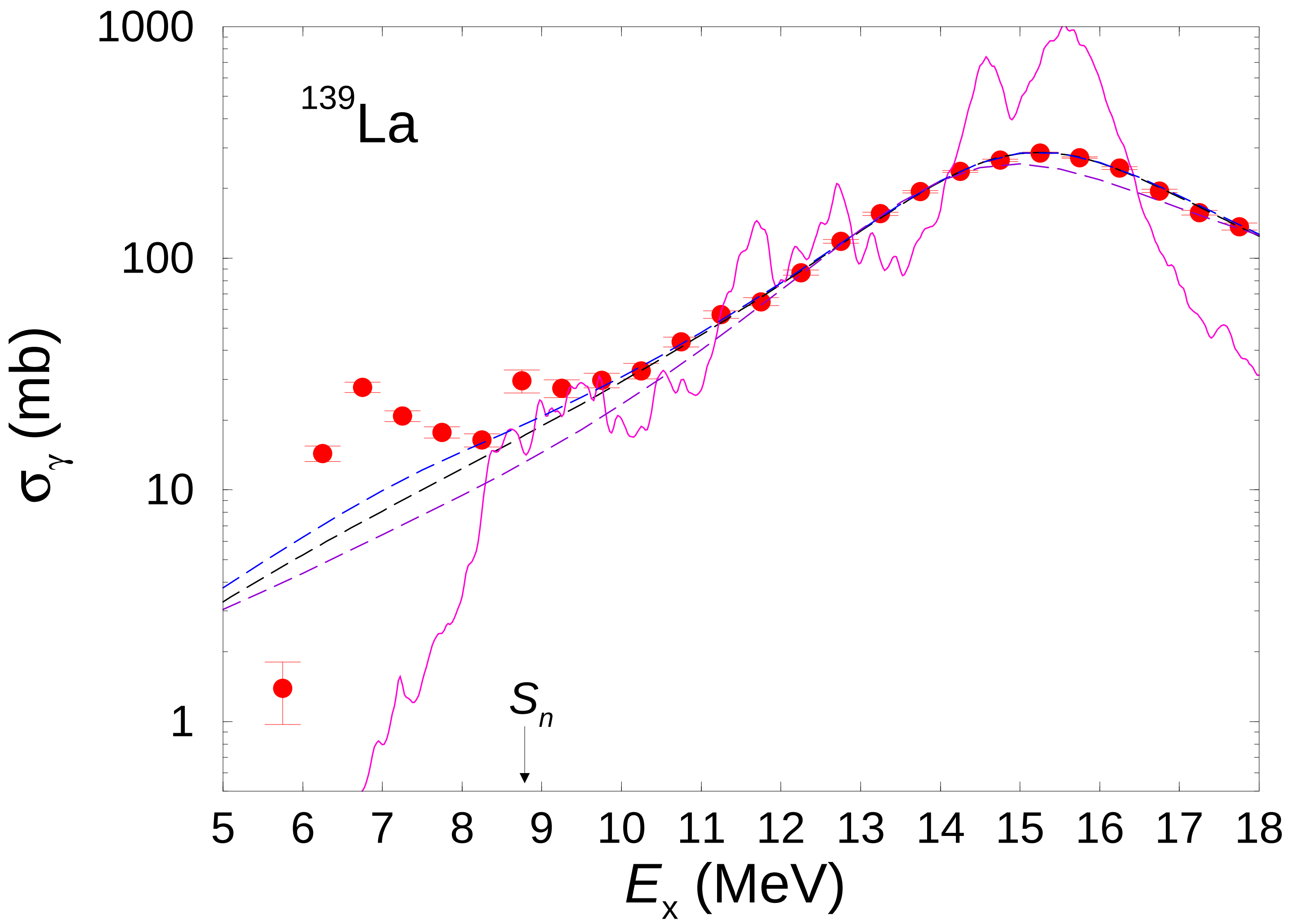

Present (γ,γ) data
$+ (\gamma, n)$ data

Lorentz curve:

$E_0 = 15.24$ MeV

$\Gamma = 4.47$ MeV

$\frac{\pi}{2}\sigma_0\Gamma = 60 \frac{NZ}{A}$ MeV mb

SLO + M1

GLO + M1

ISS-QRPA
[PRC 80, 021307R (2009)]

Absorption cross section of ^{139}La

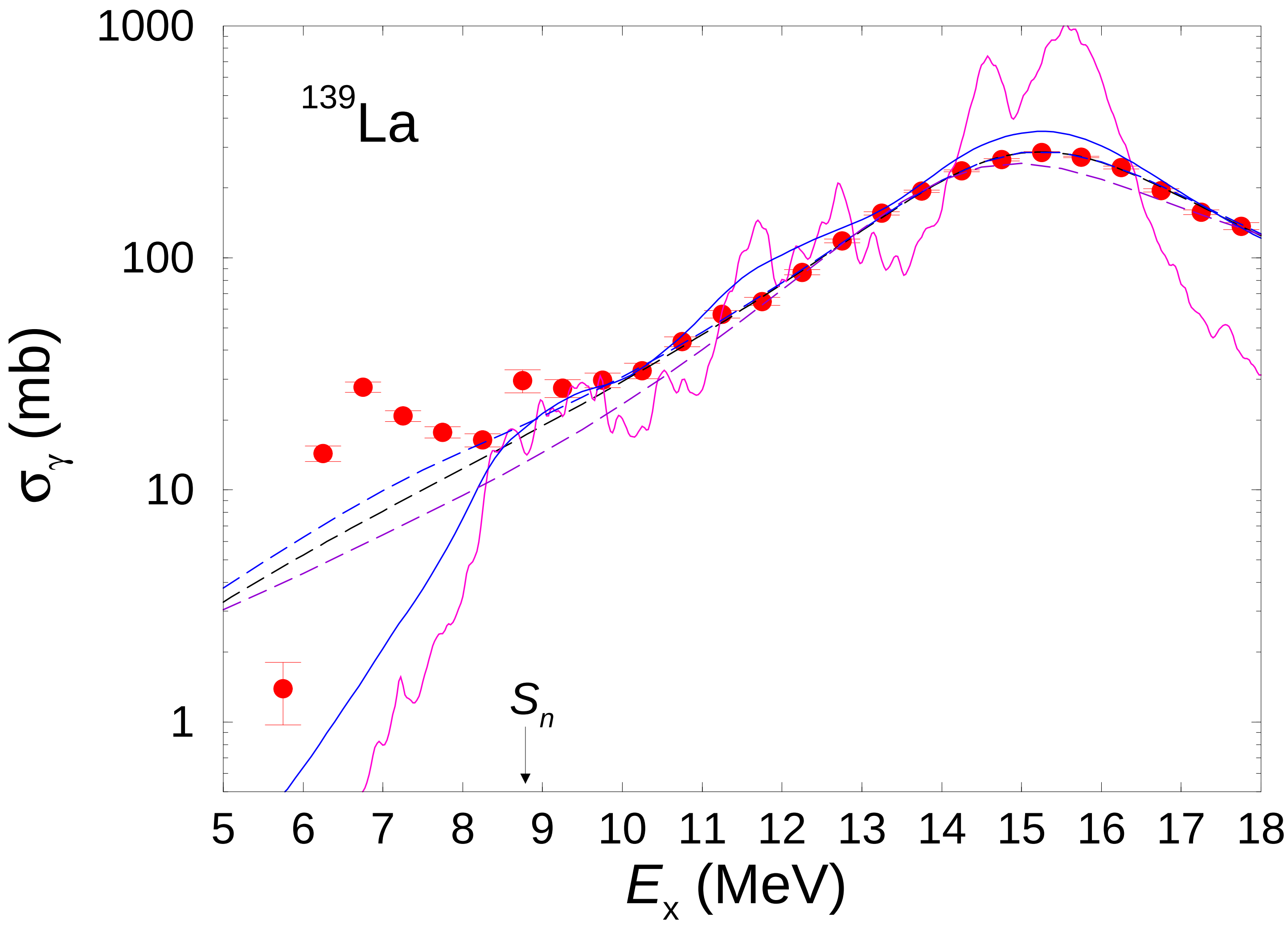

Present (γ, γ) data
$+ (\gamma, n)$ data

Lorentz curve:

$E_0 = 15.24$ MeV

$\Gamma = 4.47$ MeV

$\frac{\pi}{2}\sigma_0\Gamma = 60\ \frac{NZ}{A}$ MeV mb

SLO + M1

GLO + M1

ISS-QRPA
[PRC 80, 021307R (2009)]
$\Gamma \propto E$

Dipole strength in ^{208}Pb within the shell model

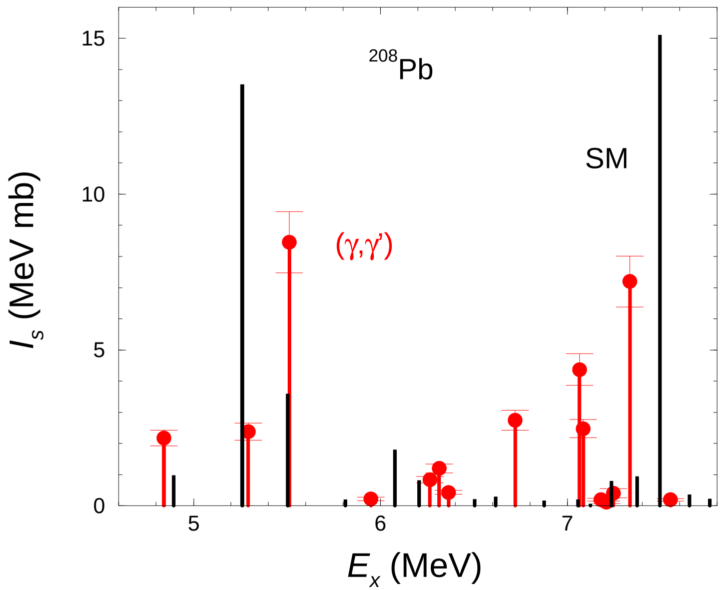

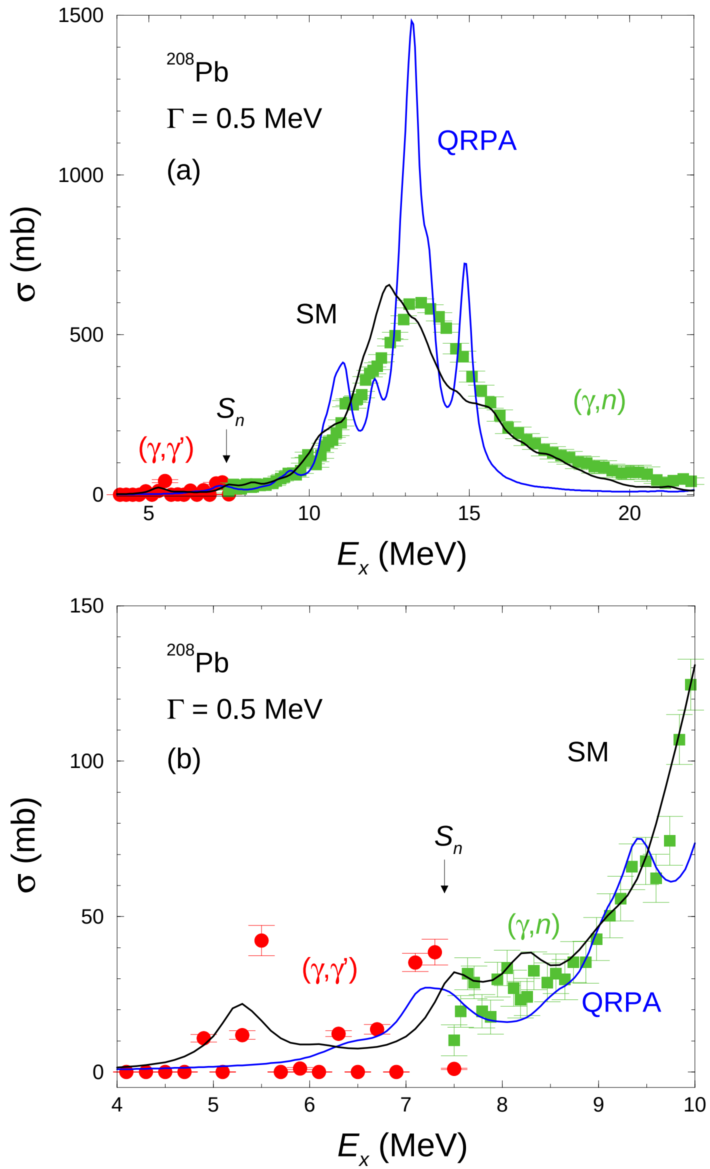

Photon-scattering at ELBE
(γ,n) data from NPA 159, 561 (1970)
Shell-model calculations
including (2p-2h) excitations
by B.A. Brown

R.S. et al., PRC 81, 054315 (2010)

Summary

- Study of dipole-strength distributions at high excitation energy and high level density via photon scattering.
- Simulations of statistical γ cascades: Estimate of intensities of inelastic transitions and correction of intensities of elastic transitions:
  - Reliable determination of σ_γ up to the neutron-separation energy S_n including unresolved strength.
  - Combination with (γ,p) and (γ,n) data gives information on σ_γ over the whole energy range from low excitation energy up to the giant dipole resonance.
  - Observation of extra strength in the range from 6 to 12 MeV – not described in phenomenological approximations of dipole-strength functions.
- Instantaneous-shape sampling combined with QRPA used to describe the dipole strength in transitional nuclei.
- Shell-model calculations including (2p-2h) excitations describe the spreading of the GDR in ^{208}Pb.
- Further developments are necessary to reproduce the extra strength below S_n.

Calculation of photonuclear and radiative-capture cross sections with TALYS

⇒ Use of experimental absorption cross sections:

- $E_\gamma > S_n$ (GDR region):
  (γ, n) data, multiplied with 0.85 according to B.L. Berman et al., PRC 36, 1286 (1987)
- ≈ 4 MeV $< E_\gamma < S_n$:
  absorption cross sections from photon-scattering experiments at ELBE
- $E_\gamma < 4$ MeV:
  calculated with three-Lorentz approximation according to
  A.R. Junghans et al., PLB 670, 200 (2008)
  deformation parameters for Mo isotopes taken from
  G. Rusev et al., PRC 73, 044308 (2006)

⇒ Comparison of the results with that obtained by using standard input strength functions (SLO and GLO); GDR peaks also multiplied with 0.85.

Nuclides studied in photon-scattering experiments

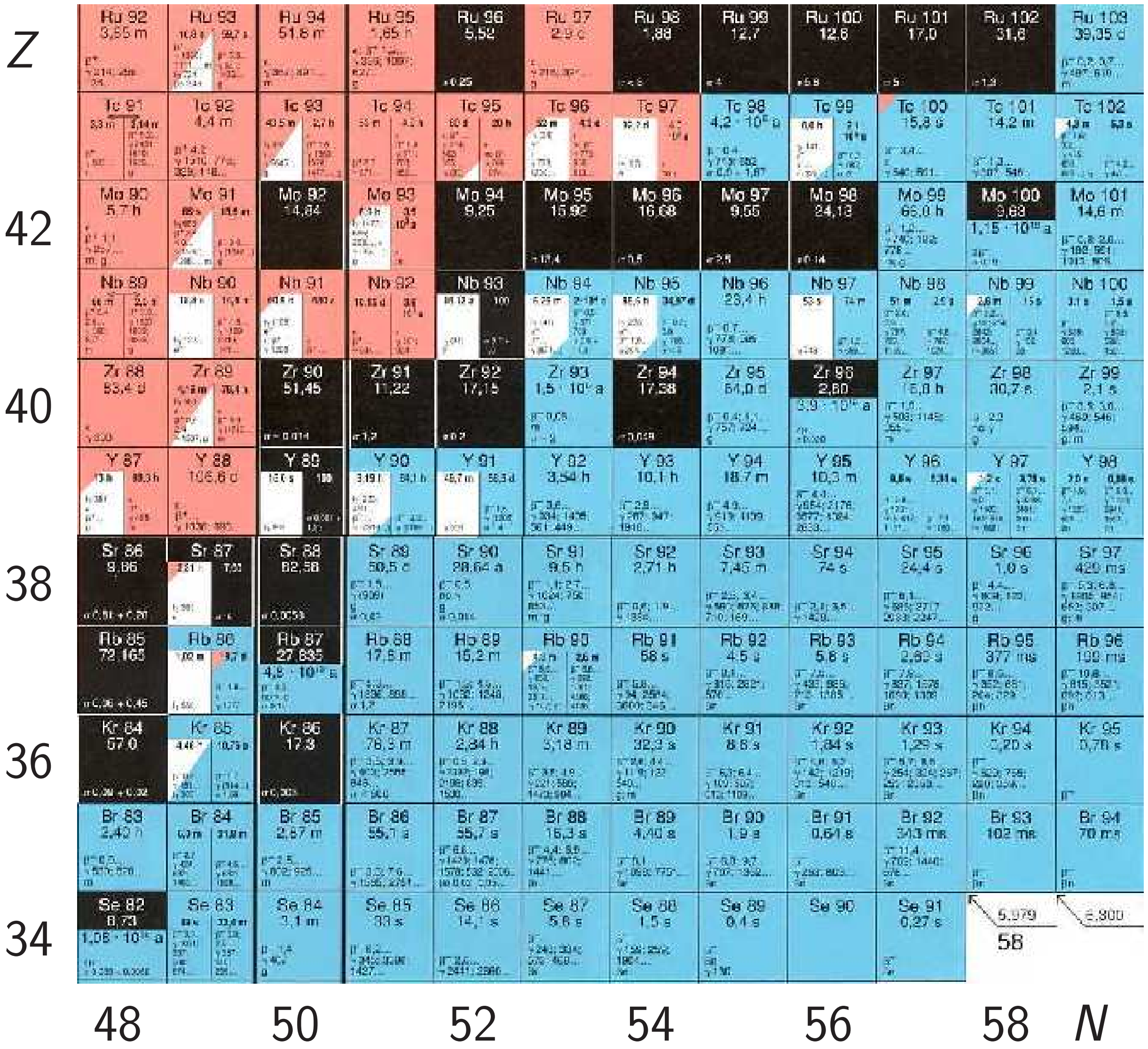

nuclide	S_n MeV	E_e^{kin} (MeV) ELBE
^{26}Mg	11.1	13.0[a]
^{92}Mo	12.7	6.0[b], 13.2[c]
^{94}Mo	9.7	13.2[c]
^{96}Mo	9.2	13.2[c]
^{98}Mo	8.6	(3.3, 3.8)[b,d], 13.2[c,e]
^{100}Mo	8.3	(3.2, 3.4, 3.8)[b,d], (7.8, 13.2)[c,e]
^{88}Sr	11.1	6.8, (9.0, 13.2, 16.0)[f]
^{89}Y	11.5	7.0, (9.5, 13.2)[g]
^{90}Zr	12.0	(7.0, 9.0, 13.2)[h]
^{139}La	8.8	11.5[i]
^{208}Pb	7.4	(9.0, 15.0)[j]

[a] R. Schwengner et al., PRC 79, 037303 (2009).
[b] G. Rusev et al., PRC 73, 044308 (2006).
[c] G. Rusev et al., PRC 79, 061302 (2009).
[d] G. Rusev et al., PRL 95, 062501 (2005).
[e] G. Rusev et al., PRC 77, 064321 (2008).
[f] R. Schwengner et al., PRC 76, 034321 (2007).
[g] N. Benouaret et al., PRC 79, 014303 (2009).
[h] R. Schwengner et al., PRC 78, 064314 (2008).
[i] A. Makinaga et al., PRC 82, 024314 (2010).
[j] R. Schwengner et al., PRC 81, 054315 (2010).

Calculation of photonuclear and radiative-capture cross sections with TALYS

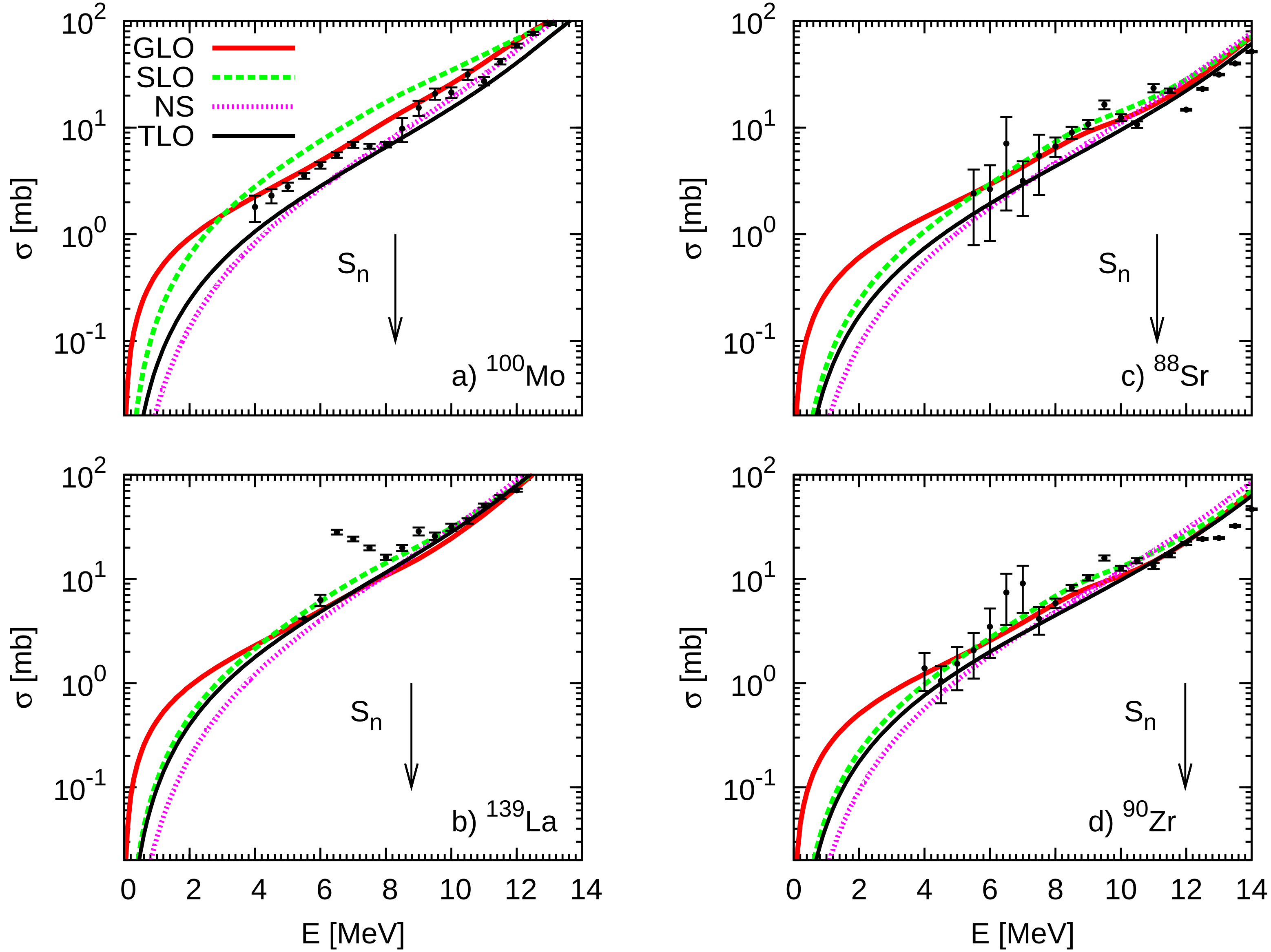

absorption cross sections

M. Beard et al.

Calculation of photonuclear and radiative-capture cross sections with TALYS

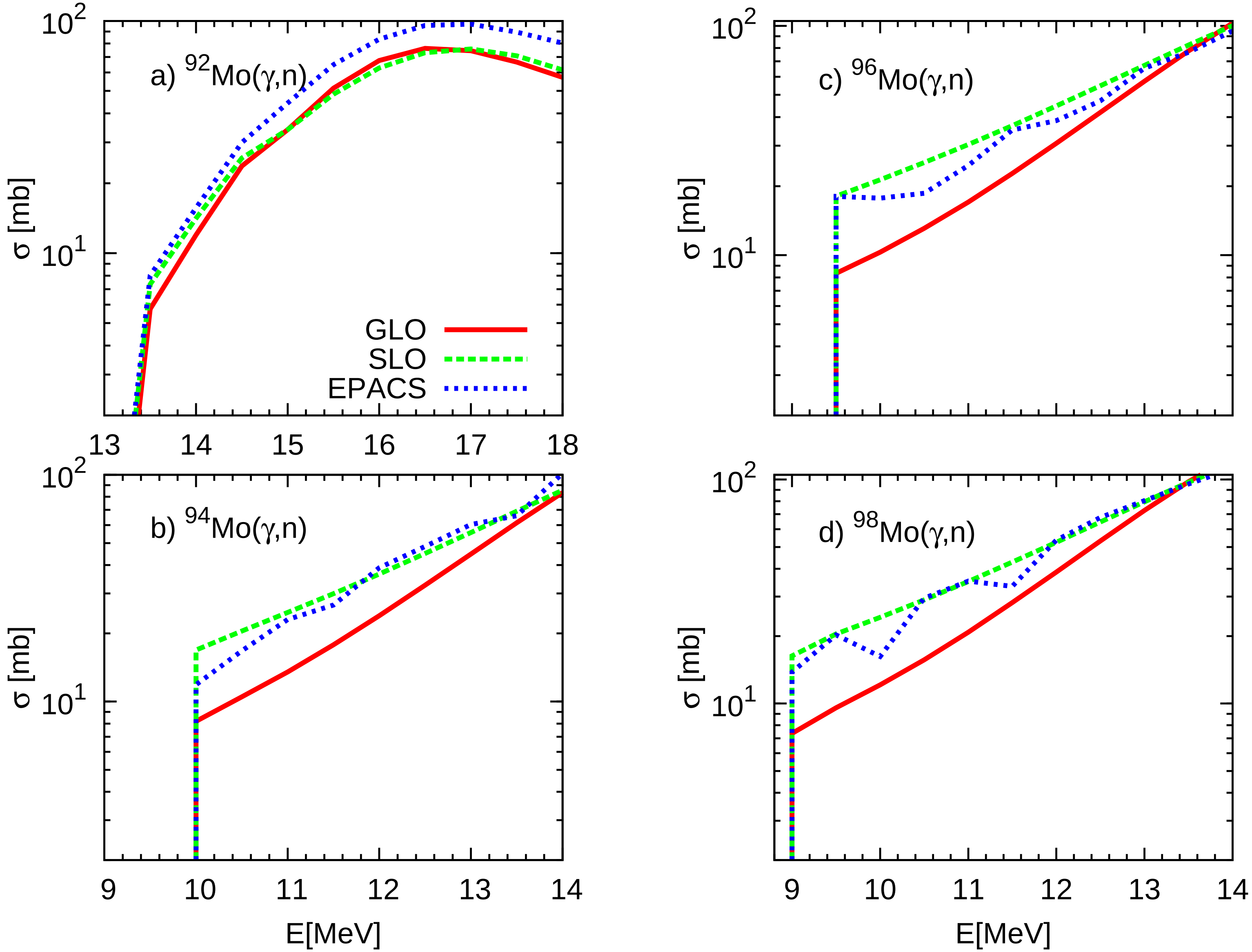

(γ, n) cross sections

M. Beard et al.

Calculation of photonuclear and radiative-capture cross sections with TALYS

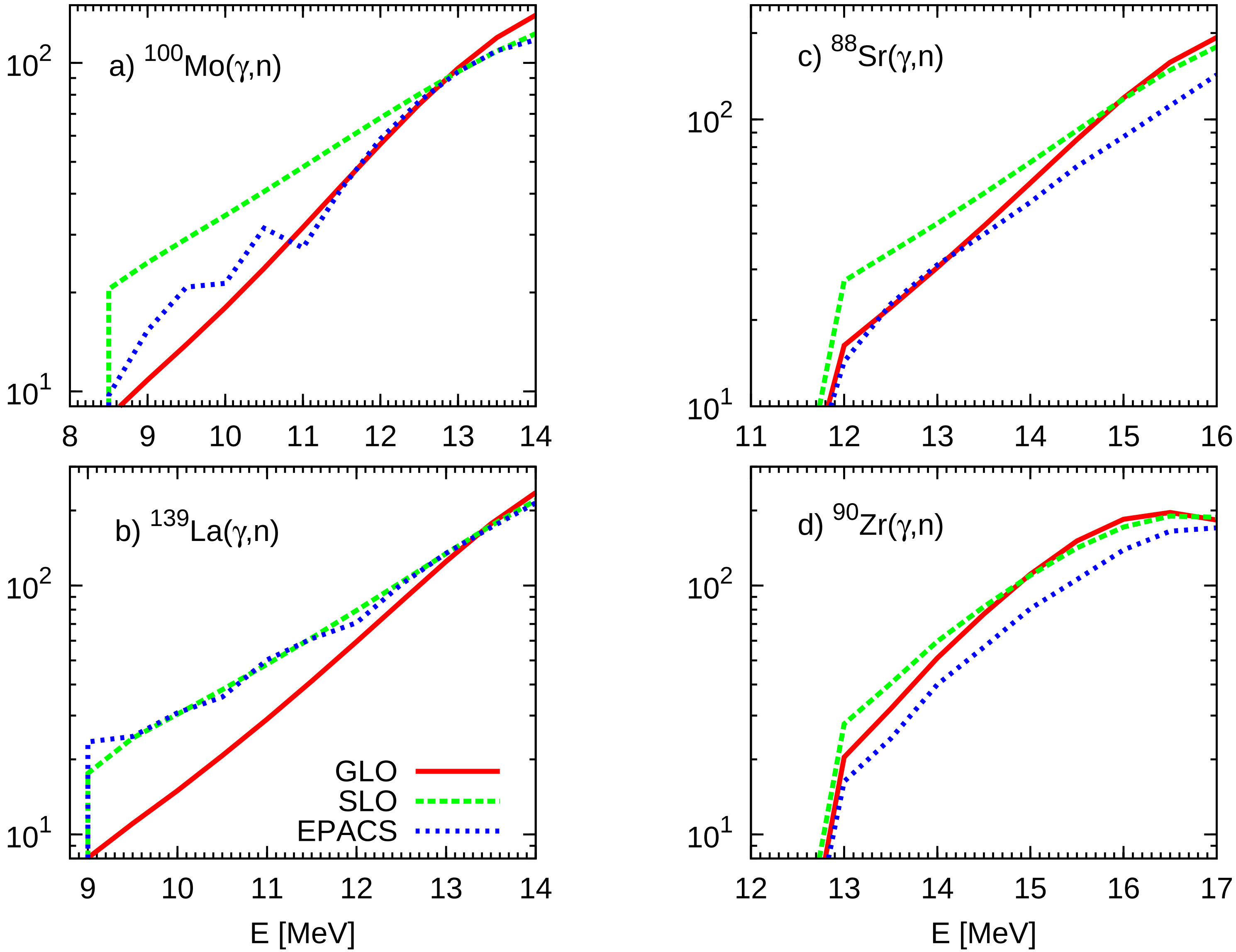

(γ, n) cross sections

M. Beard et al.

Calculation of photonuclear and radiative-capture cross sections with TALYS

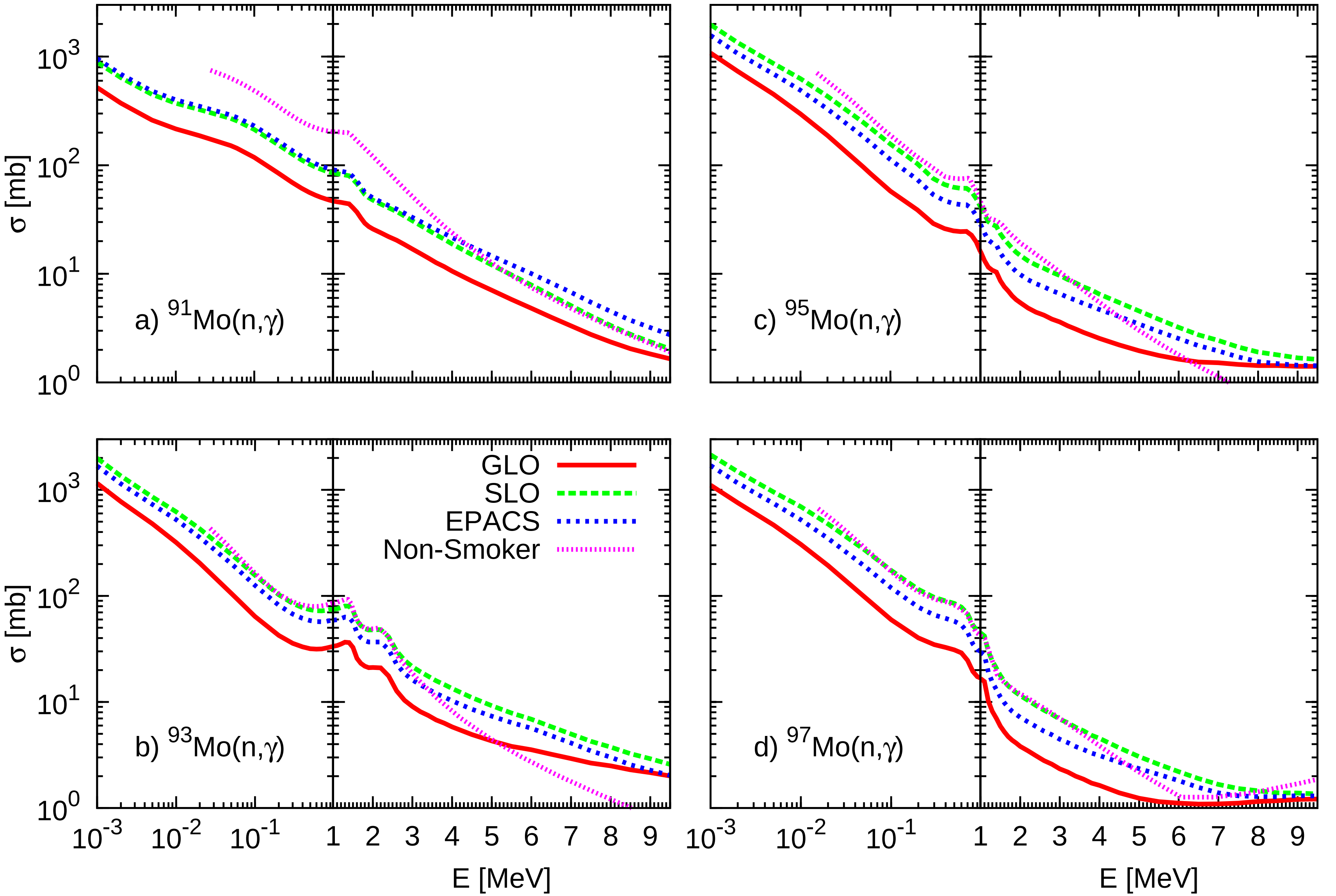

(n,γ)
cross sections

M. Beard et al.

Calculation of photonuclear and radiative-capture cross sections with TALYS

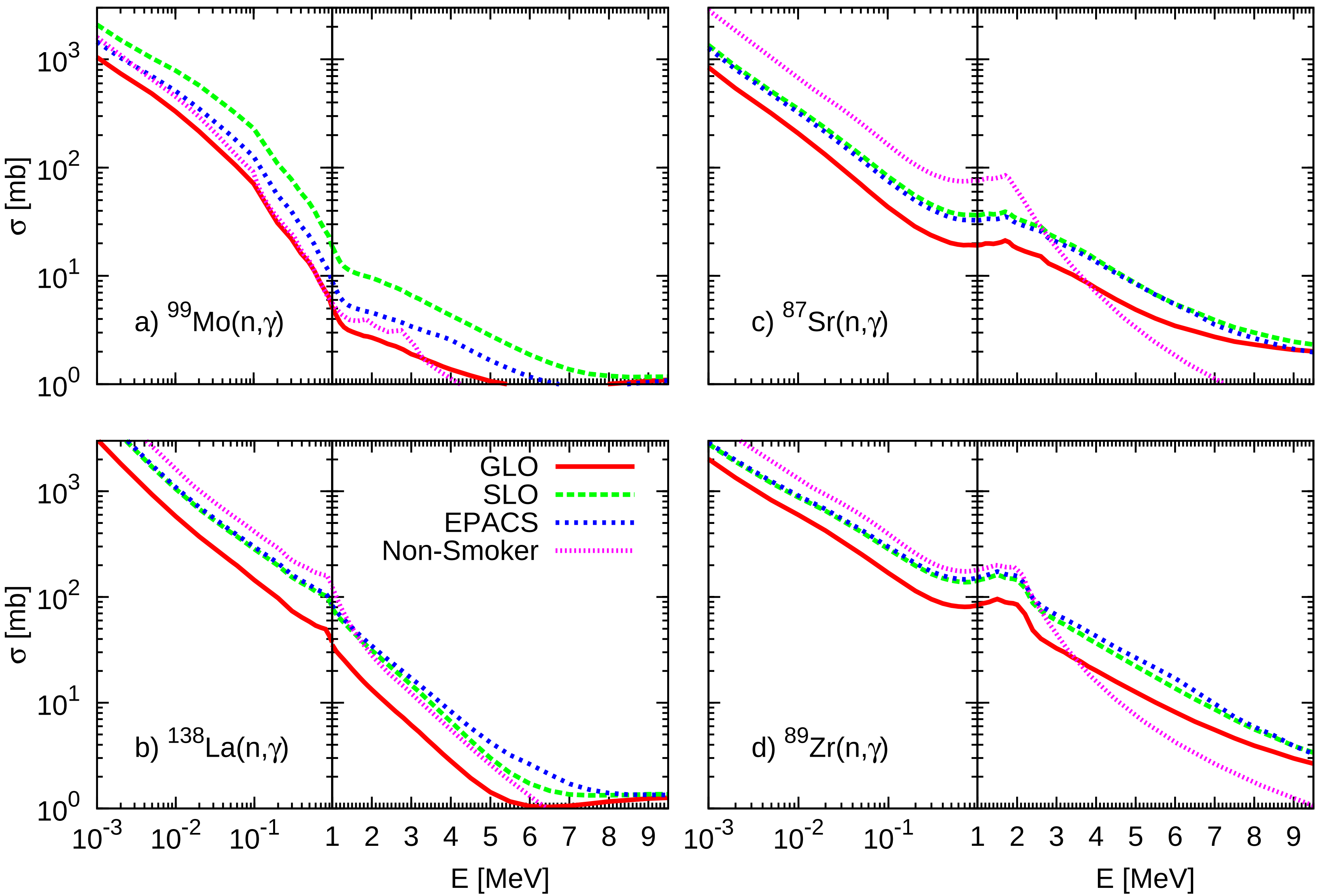

(n,γ)
cross sections

M. Beard et al.

Calculation of photonuclear and radiative-capture cross sections with TALYS

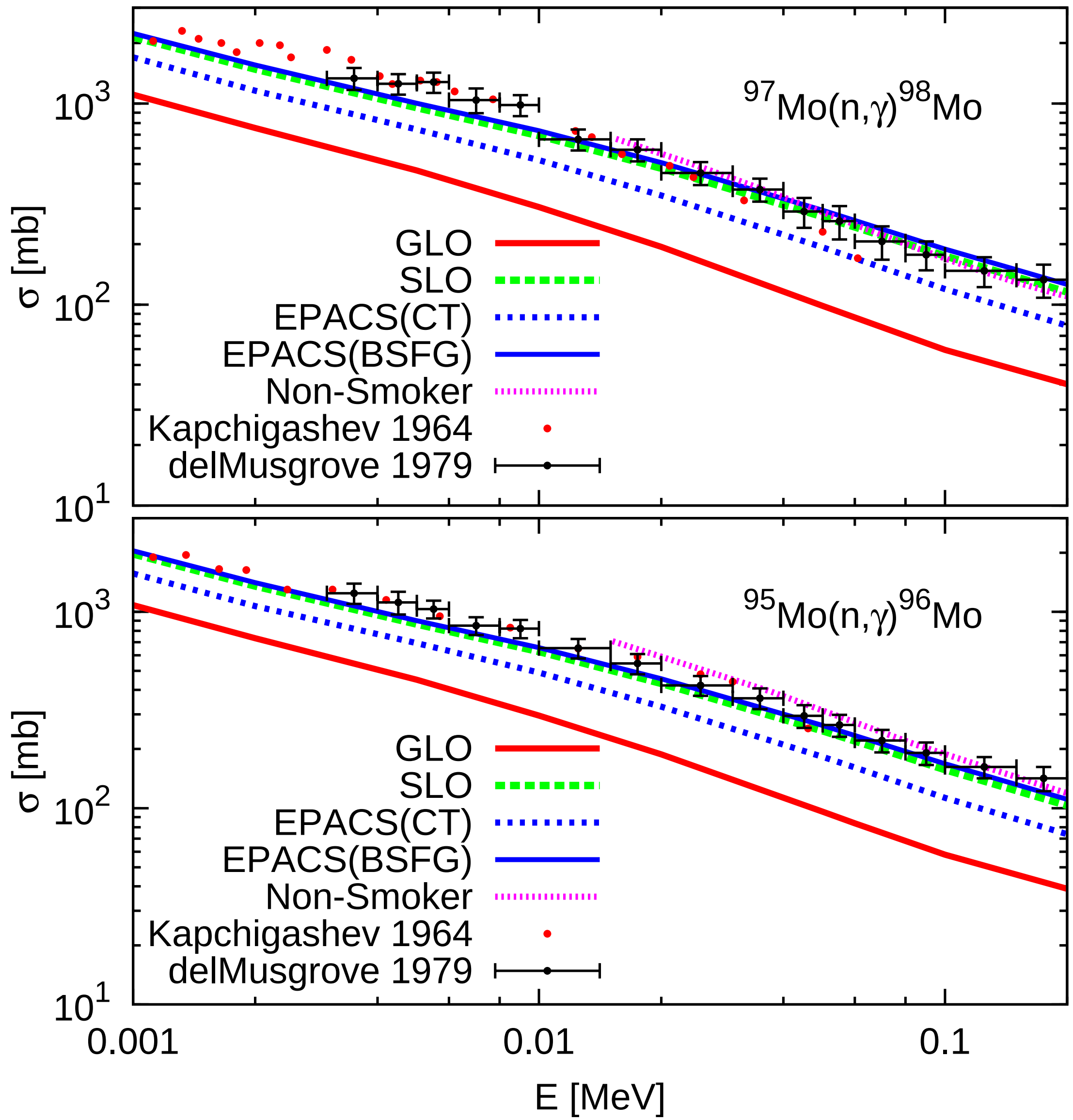

(n, γ)
cross sections

M. Beard et al.

Summary

- Calculation of photonuclear and radiative-capture cross sections with the code TALYS based on the statistical reaction model.
- Use of realistic input strength functions based on experimental photoabsorption cross sections (EPACS).
- Test of analytic expressions for strength functions as used in codes based on the statistical model and as provided by nuclear-reaction data bases.
- The EPACS results agree in most cases relatively well with the predictions using the standard-Lorentz (SLO) model, but differ from those using the Generalized-Lorentz (GLO) model.
- The enhancement of strength observed in the energy range from about 5 to 10 MeV has impact on neutron-capture cross sections for nuclides in which it is especially pronounced such as ^{139}La.

Photodissociation

Photodissociation reactions:

- (γ, n)
- (γ, p)
- (γ, α)

Method: photoactivation

- $(A, Z) + \gamma \Rightarrow (A, Z-1) + p$
- Measure decay rate of $(A, Z-1)$

$$N_{\text{act}}(E_{\text{e}}) = N_{\text{tar}} \cdot \int_{E_{\text{thr}}}^{E_{\text{e}}} \sigma_{(\gamma,x)} \; \Phi_{\gamma}(E, E_{\text{e}}) \; dE$$

$$N_{\text{act}}(E_{\text{e}}) = I_{\gamma}(E_{\gamma}) \cdot \varepsilon^{-1}(E_{\gamma}) \cdot p^{-1}(E_{\gamma}) \cdot \kappa_{\text{corr}}$$

Photoactivation of ^{92}Mo

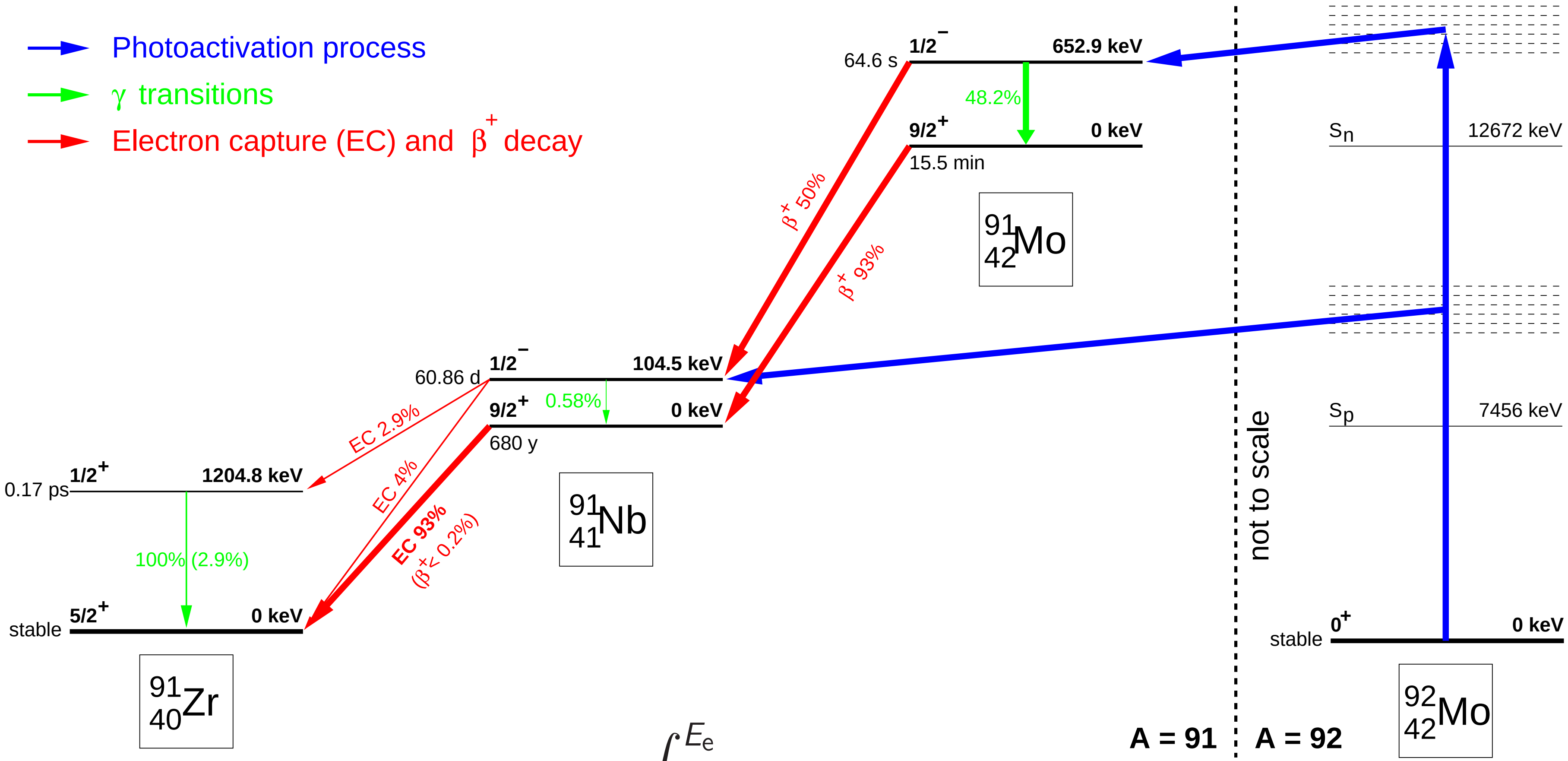

$$N_{act}(E_e) = N_{tar} \cdot \int_{E_{thr}}^{E_e} \sigma_{(\gamma,x)} \; \Phi_\gamma(E, E_e) \; dE$$

$$N_{act}(E_e) = I_\gamma(E_\gamma) \cdot \varepsilon^{-1}(E_\gamma) \cdot p^{-1}(E_\gamma) \cdot \kappa_{corr}$$

Setup for photoactivation experiments

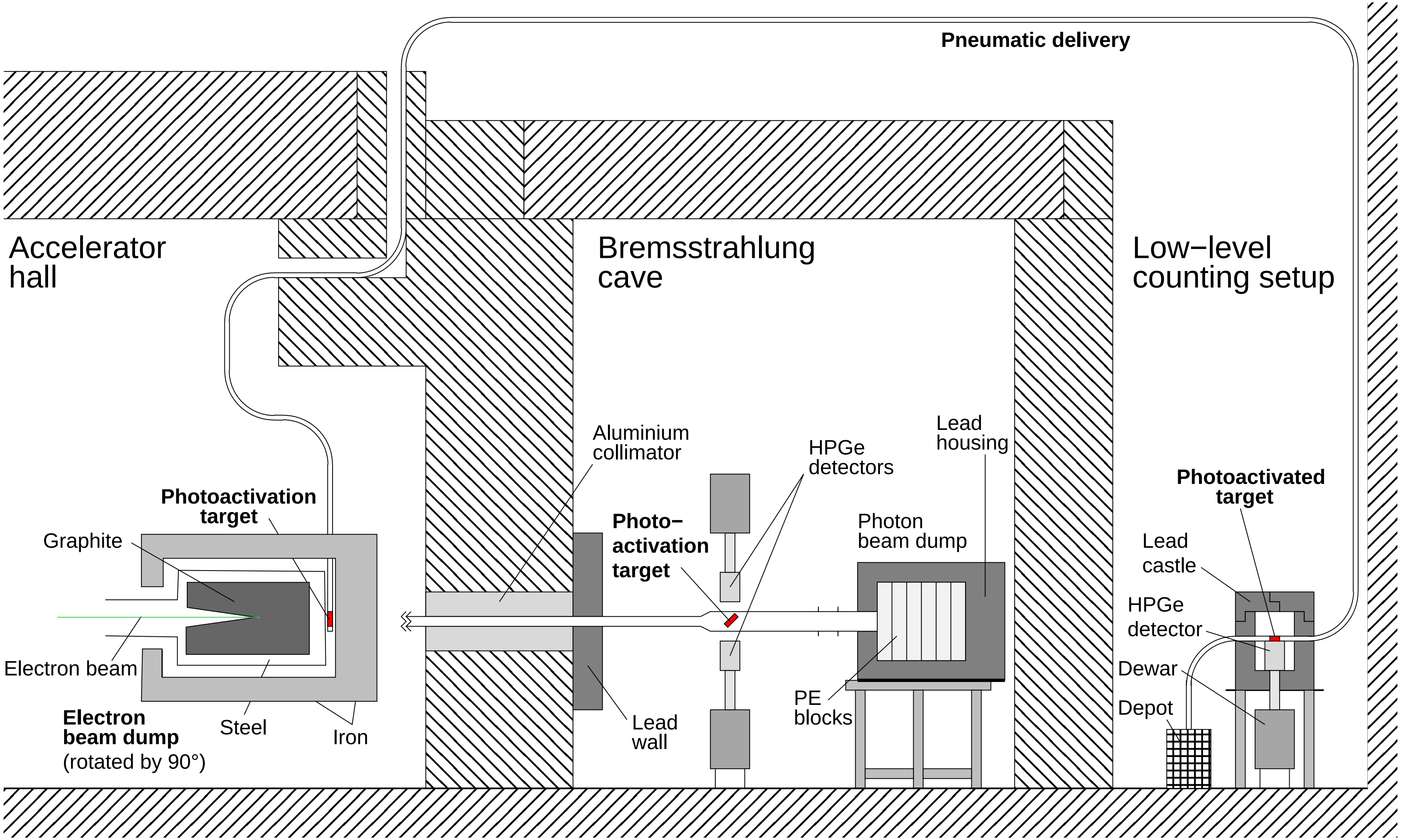

Activation yield

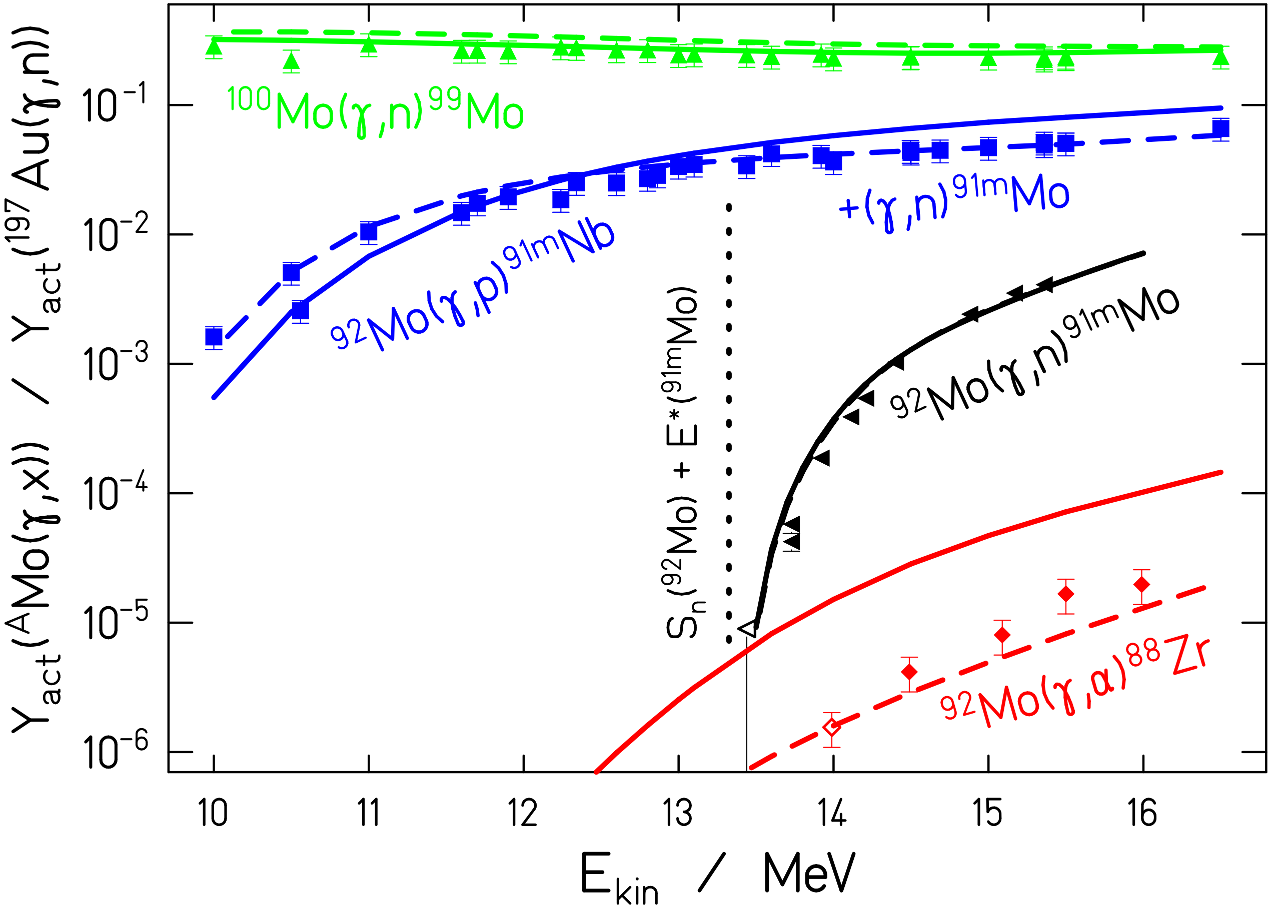

Solid lines: NON-SMOKER,
T. Rauscher and F.-K. Thielemann,
ADNDT 88, 1 (2004)

Dashed lines: TALYS,
A. Koning et al.,
AIP Conf. Proc. 769, 1154 (2005)

Activation yields of Mo isotopes normalised to the activation yield of the ^{197}Au(γ, n) reaction.

C. Nair et al., PRC 78, 055802 (2008)
M. Erhard et al., PRC 81, 034319 (2010)

Activation yield

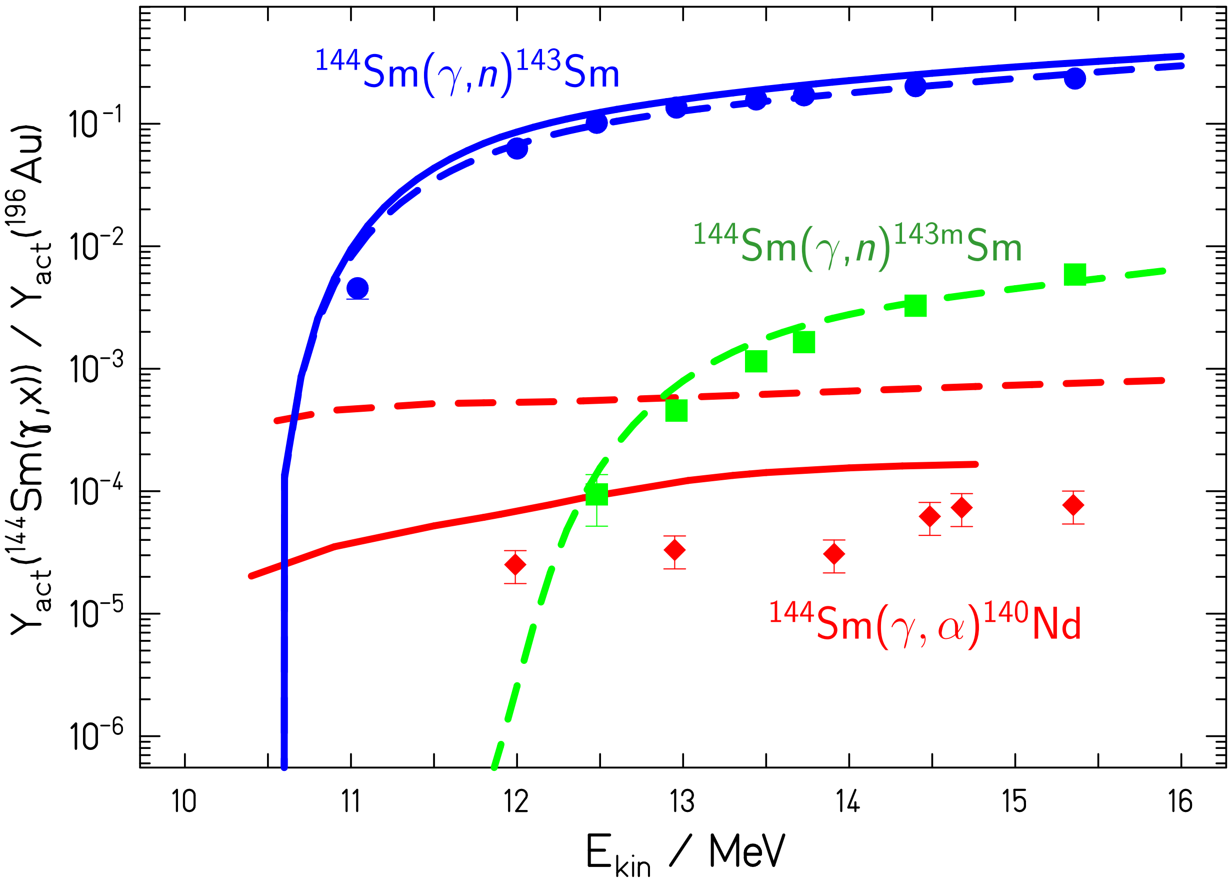

Solid lines: NON-SMOKER,
T. Rauscher and F.-K. Thielemann,
ADNDT 88, 1 (2004)

Dashed lines: TALYS,
A. Koning et al.,
AIP Conf. Proc. 769, 1154 (2005)

Activation yields of ^{144}Sm normalised to the activation yield of the ^{197}Au(γ, n) reaction.

C. Nair et al., PRC 78, 055802 (2008)
C. Nair et al., PRC 81, 055806 (2010)

Activation yield – low-background measurement

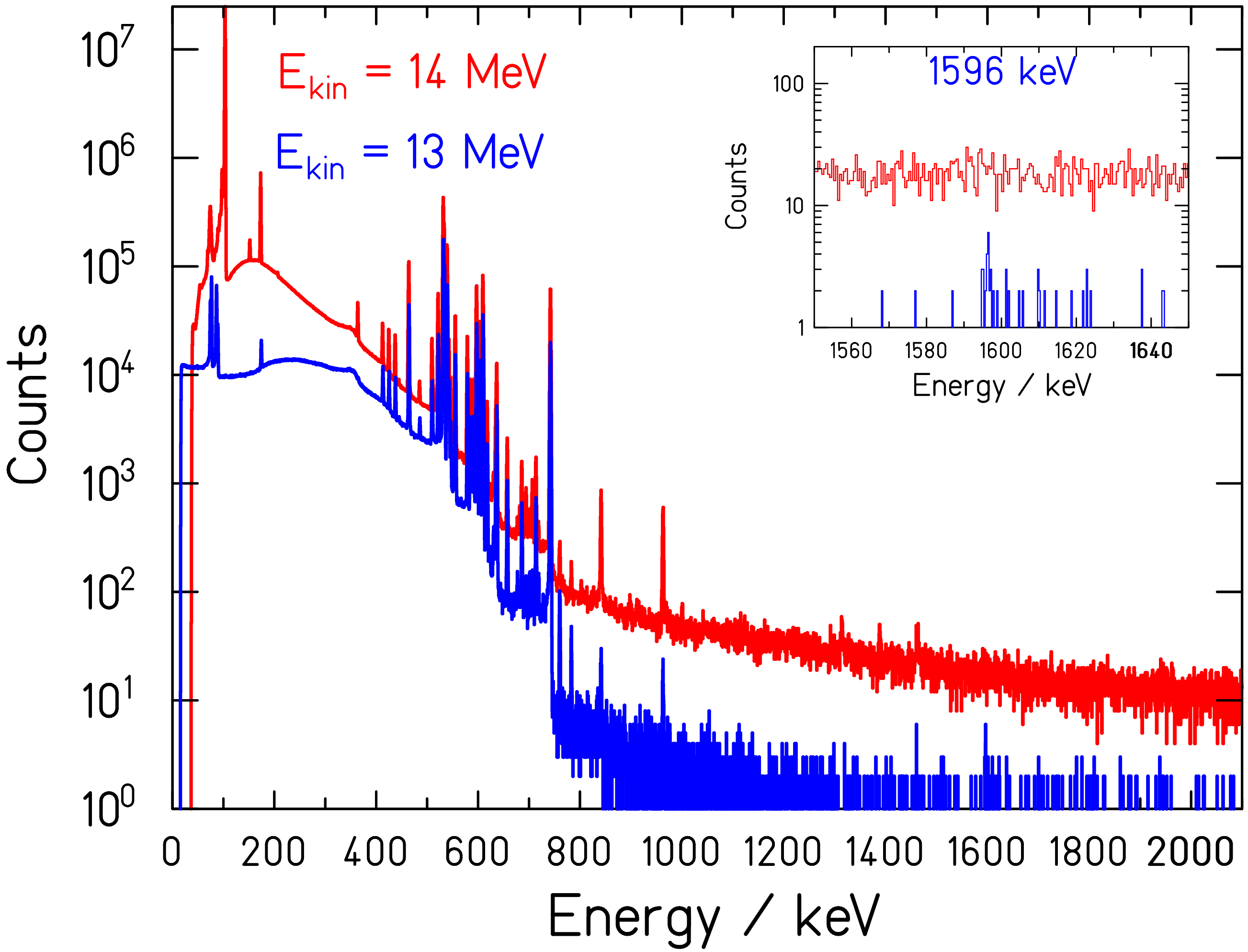

Spectra of the decay of ^{140}Nd $\longrightarrow$ ^{140}Pr $\longrightarrow$ ^{140}Ce following the ^{144}Sm(γ,α) reaction.

Measured in ELBE building

Measured in underground lab "Felsenkeller" in Dresden

Summary

- Photodissociation of Mo isotopes and of ^{144}Sm studied via photoactivation at the ELBE accelerator.
- Determination of the photon flux in the electron-beam dump by means of the ^{197}Au(γ, n) reaction.
- Measurement of weak decay rates in an underground lab.
- ^{92}Mo(γ, α)^{88}Zr and ^{144}Sm(γ, α)^{140}Nd reactions observed for the first time at astrophysically relevant energies.
- Rough agreement with predictions of Hauser-Feshbach models for (γ, n) and (γ, p) reactions. Predictions differ for (γ, α) reactions.

HZDR

Collaborators

Data analysis - photon scattering:	R. Massarczyk (HZDR) G. Rusev (TUNL and Uni Durham)
Data analysis - photoactivation:	M. Erhard (HZDR, now at PTB) C. Nair (HZDR, now at Argonne) A. Junghans (HZDR)
ISS-QRPA calculations:	F. Dönau (HZDR) S. Frauendorf (Uni Notre Dame)
Calculations of reaction rates:	M. Beard (Uni Notre Dame)
Data acquisition:	A. Wagner (HZDR)
Experiments:	D. Bemmerer (HZDR) N. Benouaret (Uni Alger) R. Beyer (HZDR) E. Birgersson (HZDR) E. Grosse (HZDR) R. Hannaske (HZDR) K. Kosev (HZDR) A. Makinaga (Uni Sapporo) M. Marta (HZDR, now at GSI) K.-D. Schilling (HZDR)